BULLETIN OF THE EARTHQUAKE
RESEARCH INSTITUTE
Vol. 57 (1982), pp. 1-47

1. The Variable Period Hypothesis and Q of the Chandler Wobble Reexamined.

By Shuhei OKUBO*,

Geophysical Institute, University of Tokyo.

(Received February 16, 1982)

Abstract

The Chandler wobble is one of the elastic-gravitational normal modes of the Earth. The eigenperiod is about 435 sidereal days, larger than the other modes by a factor 10^4, which gives the Chandler wobble an exotic status in the group of normal modes. The quality factor of the Chandler wobble, Q_w, plays a critically important role in discussing the mantle rheology since the frequency dependence of the mantle Q is affected more seriously by the low frequency Chandler Q_w than by the other seismic Q's.

A problem should be resolved in advance so as to estimate Q_w safely from the spectral analysis of the polar motion. Namely, significance of the variable Chandler period hypothesis. We test the hypothesis in two ways. First, we reexamine throughly the observational grounds of the hypothesis by applying the same scheme as employed by the proponents of the hypothesis to synthetic polar motion of a constant Chandler period. It is revealed that most of the evidence for the hypothesis is not definitive and it is also explained by the invariant Chandler period model as well. Next, we trace the time variation of the spectral structure of the Chandler wobble. For this purpose, we extend the high-resolution Instantaneous Frequency Analysis to be applicable to a complex-valued time series. Applying the technique to IPMS and BIH polar motion data, we find that the result favors the time-invariant Chandler period model.

After confirming that there is no observational difficulty in the time-invariant Chandler period model, we estimate Q_w by critically applying Maximum Entropy Spectral Analysis (MESA) to ILS and IPMS data. It is found that Q_w lies in the range of $50 \leqq Q_w \leqq 100$ and Graber's result of $Q_w=600$ is due to the erroneous choice of the length of the prediction error filter.

Finally, we discuss the effect of the mantle anelasticity upon the period and Q of the Chandler wobble. We calculate the complex

* present address: Earthquake Research Institute

Love number k for the realistic Q models by Rayleigh's principle and relate it to Q_w. The ratio of Q_w to lower mantle Q_m is found to be about 1.5 and it is shown to be consistent with the energy budget arguments. If the Chandler wobble energy is totally dissipated in the mantle, Q_m should be frequency-dependent to account for the observed Q_w of 50~100. If the frequency dependence of Q_m is the power law, the power exponent is found to be 0.1~0.2. Anelasticity of the mantle is shown to lengthen the theoretical Chandler period by 7~11 days due to physical dispersion. Adding 29.8 days of ocean effect to the theoretical period of oceanless Earth yields 438~443 sidereal days as the Chandlerian period, in excellent agreement with the observed one.

1. Introduction

The Chandler wobble is a free vibration of the Earth's rotational axis around the figure axis (MUNK & MACDONALD, 1960). Its geometrical expression is given by the Poinsot representation (Fig. 1a, b). The angular momentum axis H is fixed in space in the absence of external torques. The Earth is attached to the outer cone (body cone), and its figure axis x_3 rotates about the instantaneous rotation axis ω with a nearly diurnal period. As the body cone swings around the H axis keeping contact with the inner cone (space cone), the instantaneous rotation axis ω oscillates around the Earth's figure axis (Fig. 1c, d). This is the wobble and it is observed astronomically as latitude variation.

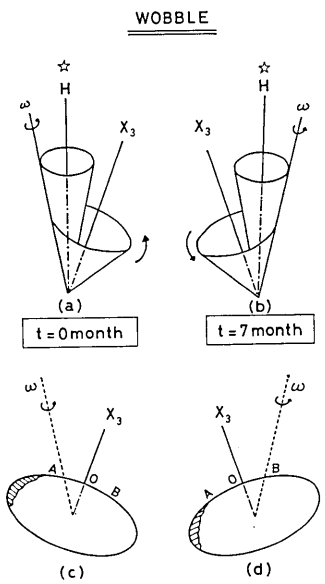

Fig. 1. (a), (b) Poinsot representation of the Chandler wobble. (c), (d) Spatial configurations of the Earth corresponding to (a) and (b).

The period and Q of the Chandler wobble are two of the most fundamental parameters that constrain the elastic and possibly anelastic properties of the solid Earth. Realizing the geophysical importance of these two parameters, numerous investigators have tried to determine those values as accurately as possible (RUDNICK, 1956; JEFFREYS, 1968; CURRIE, 1974; OOE, 1978). According to these researchers, the Chandler period is about 435 sidereal days (ROCHESTER, 1973; LAMBECK, 1980), and it is quantitatively explained by applying the elastic-gravitational normal

mode theory to realistic Earth models and assuming the equilibrium pole tide (DAHLEN, 1976 ; SMITH, 1977 ; SASAO, OKUBO & SAITO, 1980 ; SMITH & DAHLEN, 1981). However, there is a fierce controversy among researchers whether the Chandler period is steady or variable in time (Table 1). Not a few authors, including Chandler himself, postulated multiple or variable period hypothesis (CHANDLER, 1892 ; MELCHIOR, 1957 ; SEKIGUCHI, 1972, 1976 ; GAPOSCHKIN, 1972 ; CARTER, 1981), but they are not yet confirmed because of the dubious nature of the analytical technique. It is rather astonishing that the hypothesis has survived nearly 90 years without either being completly rejected or confirmed. One of the objects of this study is to draw conclusion on this problem.

Table 1. History of the controversy on the variable/multiple Chandler period.

variable/multiple		invariant/single	
Chandler	(1892)	Newcomb	(1892)
Kimura	(1918)		
Hattori	(1949)		
Melchior	(1957)	Munk & MacDonald	(1960)
Colombo & Shapiro	(1968)		
Gaposchkin	(1972)	Pedersen & Rochester	(1972)
Sekiguchi	(1976)	Ooe	(1978)
Carter	(1981)		

Contrary to the agreement on the estimates of the Chandler period (except for the time-variable period hypothesis), there is no consensus about the Chandler wobble Q (hereafter denoted by Q_w) (Table 2). Estimated values range from 25 to a high of 600. RUDNICK (1956) estimated $Q_w=25$ from the periodgram analysis of International Latitude Service (ILS) data of 54.4 years long. CURRIE (1974) gave $Q_w=72$ from Maximum Entropy Spectral Analysis (MESA) of ILS data of 73 year duration. GRABER (1976) also applied MESA to International Polar Motion Service (IPMS) data of 15 year long and obtained $Q_w=600$. Differences of the adopted technique and the length of analyzed data affect the estimate for Q_w considerably as shown above. The matter becomes more complicated if the time-variable Chandler period hypothesis is the case. It is expected that the ordinary harmonic analysis of the polar motion with a variable period and higher Q_w ($Q_w \gg 100$) would yield apparently lower Q_w value ($Q_w < 100$). Since the frequency dependence of the mantle Q (hereafter

Table 2. Previous estimates of the Chandler wobble Q.

$Q_w<30$	$50<Q_w<100$	$Q_w>500$
Rudnick (1956)	Jeffreys (1968)	Graber (1976)
Walker & Young (1957)	Claerbout (1969)	
	Currie (1974)	
Munk & MacDonald (1960)	Wilson & Haubrich (1976)	
	Ooe (1978)	

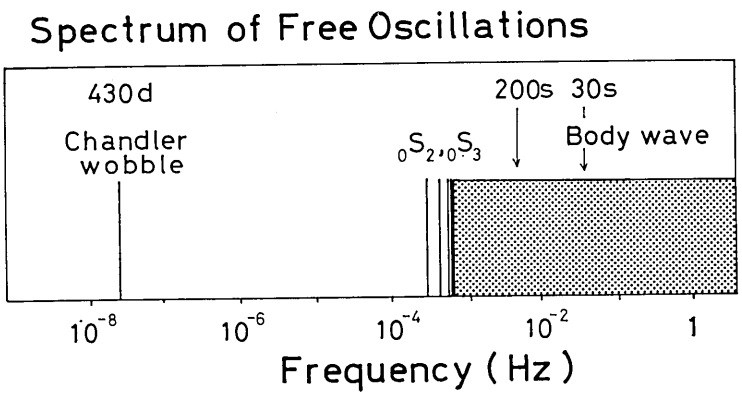

Fig. 2. Schematic line spectrum of the Earth's elastic-gravitational normal modes.

denoted by Q_m) is often discussed based upon the estimate of Q_w, an accurate determination of Q_w is critically important (ANDERSON & MINSTER, 1979) (Fig. 2).

In summary, models of the Chandler wobble can be classified into three groups.

(1) Multiple or variable Chandler period with a high Q_w ($Q_w \gg 100$).
(2) Single Chandler period with a high Q_w ($Q_w \gg 100$).
(3) Single Chandler period with a low Q_w ($Q_w < 100$).

In this paper, we will test all the evidence which seems to support the variable period hypothesis and show that it is also explained by the model (3). In order to test the hypothesis more directly, we trace the time-variation of the spectral structure of the polar motion. For this purpose, we extend the Instantaneous Frequency Analysis to be applicable to a complex-valued time series, The result does not reveal significant fluctuation of the Chandlerian period and favors the invariant period model.

After confirming that there is no observational obstacle to the invariant Chandler period model, we can safely estimate Q_w from the spectral analysis of the polar motion. The most favorable value is found to be $50 \leqq Q_w \leqq 100$ from the simulation approach of MESA. We will also elucidate the cause of the wide discrepancy between the estimated Q_w's by the previous authors.

If the wobble energy is totally dissipated within the mantle, some relation should hold between Q_w and Q_m at the Chandler frequency. Q_w and Q_m are defined as

$$Q_w = 2\pi E_w / \Delta E$$

$$Q_m = 2\pi E_s / \Delta E$$

where E_w and E_s are the total energy of the wobble and the strain energy, respectively. ΔE is the amount of energy dissipated in one cycle of the oscillation. E_w is larger than E_s since E_w includes the kinetic, the gravitational and the strain energies. Hence Q_m is smaller than Q_w. Most of the earlier investigators supposed $E_w \cong 10 \cdot E_s$ from the kinematical arguments and obtained $Q_w \cong 10 \cdot Q_m$ (STACEY, 1969, 1977; MERRIAM & LAMBECK, 1979). However, we find that E_w/E_s is at most 2 and Q_w/Q_m is also $1 \sim 2$ from the more rigorous treatment. We confirm the result by computing the complex Chandler frequency for the realistic Earth models with complex elastic moduli by Rayleigh's principle. Using the relation between Q_m and Q_w and the observed Q_w value, the frequency dependence of the mantle Q will be discussed.

Anelasticity of the mantle induces what is called physical dispersion. Hence the elastic moduli (real part) at the Chandler frequency is different from those appropriate for the seismic frequency range. We will assess the effect of physical dispersion on the Chandler period and show that the Chandler period is lengthend by about $7 \sim 11$ days.

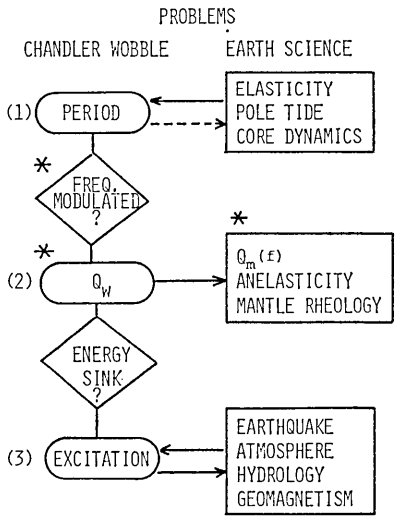

Fig. 3. Schematic diagram on the problems concerning the Chandler wobble. * denotes the aim in this study.

2. Formulation of the Earth's rotation

§ 1. Derivation of the basic wobble equation

The rotation of the Earth is a complicated problem owing to its

radially inhomogeneous structure and the presence of the fluid outer core. We shall briefly review the formulation of the rotation dynamics of the oceanless, slightly elliptical, realistic Earth after SASAO, OKUBO & SAITO (1980).

(1) Basic state

We use a reference frame fixed to the mean principal axes of the mantle rotating with an angular velocity $\vec{\omega}$.

$$\vec{\omega}=\Omega(m_1, m_2, 1+m_3)$$

We take $\vec{i}_1$, $\vec{i}_2$ and $\vec{i}_3$ as the basis vectors in this frame. The hydrostatic equilibrium state in the fluid core is expressed as

$$\nabla P_0=\rho_0\nabla\phi_0$$

where P, ρ and ϕ denote the pressure, the mass density and the gravitational potential (including centrifugal potential), respectively. Subscript 0 designates the basic state. We assume the coincidence of the equipotential and equidensity surfaces in the basic state. The distance from the origin to the surface, r_0, is given by

$$r_0=r(1-(2/3)\cdot\varepsilon(r)\cdot P_2(\cos\theta))$$

where r and θ are the distance parameter and the colatitude, respectively. $\varepsilon(r)$ is the geometrical ellipticity of the equipotential surface and P_2 is the Legendre function of degree 2.

$\varepsilon(r)$ is given by integrating the Clairaut equation.

$$\frac{d^2\varepsilon}{dr^2}-\frac{6}{r^2}\varepsilon+\frac{8\pi G\rho_0}{g_0}\left(\frac{d\varepsilon}{dr}+\frac{\varepsilon}{r}\right)=0$$

where g_0 is given by

$$g_0(r)=4\pi G\int_0^r\rho_0(b)b^2\,db/r^2$$

The boundary conditions for $\varepsilon(r)$ are

$$r\frac{d\varepsilon}{dr}+2\varepsilon=(5/2)\,\Omega^2 r/g_0 \qquad \text{at } r=a$$

$$\frac{d\varepsilon}{dr}=0 \qquad \text{at } r=0$$

(2) Velocity field in the fluid core

The velocity field in the fluid core is assumed to be composed of a uniform rotation and a small correcting term $\vec{v}$.

$$\vec{v}_f=\vec{\omega}_f\times\vec{r}+\vec{v}$$

$$\vec{\omega}_f = \Omega(m_1^f, m_2^f, m_3^f)$$

where $\vec{\omega}_f$ denotes the angular velocity of the fluid core. The hydrodynamic equations of motion and continuity for the perturbed state are given by

$$\rho_0\left(\frac{\partial \vec{v}_f}{\partial t} + \frac{d\vec{\omega}}{dt} \times \vec{r} + 2\Omega \vec{i}_3 \times \vec{v}_f\right) = -\nabla P_1 + \rho_1 \nabla \phi_0 + \rho_0 \nabla \phi_1$$

$$\frac{\partial \rho_1}{\partial t_1} + \rho_0 \nabla \cdot \vec{v}_f + \vec{v}_f \cdot \nabla \rho_0 = 0 \qquad (2\text{-}1)$$

where the subscript 1 designates the perturbed state. The Poisson equation is

$$\nabla^2 \phi_1 = -4\pi G \rho_1$$

The perturbed potential is composed of three terms.

$$\phi_1 = \phi_e + \phi_m + \phi_d$$

$$\phi_e = (\Omega^2/3) r^2 \,\mathrm{Re}\,[\tilde{\rho} Y_2^1]$$

$$\phi_m = -(\Omega^2/3) r^2 \,\mathrm{Re}\,[\tilde{m} Y_2^1]$$

$$\nabla^2 \phi_d = -4\pi G \rho_1$$

where Y_2^1 is the spherical surface harmonic of degree 2, order 1. ϕ_e is the external tidal potential and ϕ_m is the pole tide potential. ϕ_d is the gravitational potential arising from the elastic deformation of the Earth. $\tilde{m}$ designates the complex representation of the wobble and is defined as

$$\tilde{m} = m_1 + i m_2$$

Introducing new quantities

$$\phi_f = -(\Omega^2/3) r^2 \,\mathrm{Re}\,[\tilde{m}_f Y_2^1] = -\Omega^2 (m_1^f xz + m_2^f yz)$$

$$\tilde{m}_f = m_1^f + i m_2^f$$

(2-1) is rewritten as

$$\frac{\partial \vec{v}}{\partial t} + \frac{d(\vec{\omega} + \vec{\omega}_f)}{dt} \times \vec{r} + 2\Omega \vec{i}_3 \times \vec{v} + \Omega(\vec{i}_3 \times \vec{\omega}_f) \times \vec{r} = -\nabla \boldsymbol{P} - \boldsymbol{R} \nabla r_0 \qquad (2\text{-}2)$$

$$\boldsymbol{P} = P_1/\rho_0 - \phi_1 - \phi_f$$

$$\boldsymbol{R} = P_1 (d\rho_0/dr_0)/\rho_0^2 - \rho_1 (d\phi_0/dr_0)/\phi_0 .$$

Multiplying (2-2) by $\rho_0 \vec{r}$ vectorically and integrating the product over the whole core, we obtain

$$\frac{d\vec{H}_f}{dt}-\vec{\omega}_f\times\vec{H}_f=-\vec{\omega}\times\int\rho_0\vec{r}\times\vec{v}dv-\int\rho_0\boldsymbol{P}\vec{r}\times d\vec{S}$$

$$+\int(\boldsymbol{P}d\rho_0/dr_0-\rho_0\boldsymbol{R})\vec{r}\times\nabla r_0 dV$$

$$\vec{H}_f=A_f(\vec{\omega}+\vec{\omega}_f)+(C_f-A_f)\Omega\vec{i}_3+c_{31}^f\Omega\vec{i}_1$$

$$+c_{32}^f\Omega i_2+\int\rho_0\vec{r}\times\vec{v}dV \tag{2-3}$$

where A_f and C_f are the least and the greatest principal moments of inertia and $-c_{31}^f$ and $-c_{32}^f$ are the products of inertia of the fluid core. We may choose $\vec{\omega}_f$ so that $\int\rho_0\vec{r}\times\vec{v}dV$ vanishes without loss of generality. SASAO, OKUBO & SAITO showed that $\boldsymbol{P}$ and $\boldsymbol{R}$ are of the order of $\Omega|\vec{v}|$ and the integrals on the right hand side of (2-3) are negligible since $\boldsymbol{P}$ and $\boldsymbol{R}$ are further multiplied by factors of order $\varepsilon(r)$. Thus we obtain

$$\frac{d\vec{H}_f}{dt}-\vec{\omega}_f\times\vec{H}_f=0 \tag{2-4}$$

(3) Basic wobble equations

The Liouville equation of the whole Earth is

$$\frac{d\vec{H}}{dt}+\vec{\omega}\times\vec{H}=\vec{L} \tag{2-5}$$

$$\vec{H}=A\vec{\omega}+(C-A)\Omega\vec{i}_3+A_f\vec{\omega}_f+c_{31}\Omega\vec{i}_1+c_{32}\Omega\vec{i}_2$$

$$\vec{L}=\int\rho_0\vec{r}\times\nabla\phi_e dV$$

Equations (2-4) and (2-5) give

$$A_f[D\tilde{m}+(D+i(1+e_f)\Omega)\tilde{m}_f]+D\tilde{c}_3^f=0$$

$$A(D-ie\Omega)\tilde{m}+(D+i\Omega)(A_f\tilde{m}_f+\tilde{c}_3)=-iAe\Omega\tilde{\phi} \tag{2-6}$$

where D stands for d/dt. e and e_f are the dynamical flattenings of the Whole Earth and the fluid core, respectively.

$$e=(C-A)/A$$

$$e_f=(C_f-A_f)/A_f$$

$\tilde{c}_3$ and $\tilde{c}_3^f$ are defined as

$$\tilde{c}_3=c_{31}+ic_{32}$$

$$\tilde{c}_3^f=c_{31}^f+ic_{32}^f$$

SASAO, OKUBO & SAITO showed that $\tilde{c}_3$ and $\tilde{c}_3^f$ arising from the elastic deformation are given by

$$\tilde{c}_{3,e}=-A[\kappa(\tilde{\rho}-\tilde{m})-\xi\tilde{m}_f]$$
$$\tilde{c}_3^{f}{}_{,e}=-A_f[\gamma(\tilde{\rho}-\tilde{m})-\beta\tilde{m}_f] \tag{2-7}$$

where κ, ξ, β and γ are the physical constants characteristic of each Earth model.
Substituting (2-7) into (2-6) yields

$$\begin{pmatrix} (1+\gamma)D & , & (1+\beta)D+i(1+e_f)\Omega \\ (1+\kappa)D+i(\kappa-e)\Omega\,, & & (A_f/A+\xi)(D+i\Omega) \end{pmatrix}\begin{pmatrix}\tilde{m}\\ \tilde{m}_f\end{pmatrix}=\begin{pmatrix}\tilde{\phi}_1\\ \tilde{\phi}_2\end{pmatrix}$$
$$\begin{pmatrix}\tilde{\phi}_1\\ \tilde{\phi}_2\end{pmatrix}=\begin{pmatrix}\gamma D\tilde{\phi}-D\tilde{c}_3'^{f}/A_f\\ \kappa D\tilde{\phi}-ie\Omega\tilde{\phi}-(D+i\Omega)\tilde{c}_3'/A\end{pmatrix} \tag{2-8}$$

where $\tilde{c}_3'$ and $\tilde{c}_3'^{f}$ are given by

$$\tilde{c}_3'=\tilde{c}_3-\tilde{c}_{3,e}$$
$$\tilde{c}_3'^{f}=\tilde{c}_3^{f}-\tilde{c}_3^{f}{}_{,e}$$

Now we can derive eigenfrequencies of the free motion by solving the secular equation. Since κ, ξ, β and γ are of order 10^{-3} or less, a first approximation for the secular equation is

$$\begin{vmatrix} \sigma & , & \sigma+\Omega \\ \sigma+(\kappa-e)\Omega\,, & & (A_f/A)(\sigma+\Omega)\end{vmatrix}=0$$
$$(\sigma+\Omega)(\sigma-A(e-\kappa)\Omega/A_m)=0 \tag{2-9}$$

where σ denotes angular frequency. A_m is the least principal moment of inertia of the mantle and it is given by

$$A_m=A-A_f\,.$$

The roots of the equation (2-9) correspond to the angular frequencies of the Chandler wobble and the free core nutation (nearly diurnal wobble). The Chandlerian angular frequency for the oceanless, perfectly elastic Earth is given by

$$\sigma_e=(A/A_m)\cdot(e-\kappa)\Omega \tag{2-10}$$

Now we shall assess the effect of oceans upon the rotation dynamics. Mobility of oceans induces variation of c_{13}' and c_{23}' synchronous to wobble due to the pole tide.

$$\tilde{c}_{3,o}'=c_{13,o}'+ic_{23,o}'=(\sigma'/\Omega)A_m\cdot\tilde{m} \tag{2-11}$$

where subscript o refers to the effect of oceans. σ' is a physical constant. Substituting (2-11) into (2-8) and solving the secular equation, we obtain

$$\sigma_c=\sigma_e-\sigma' \tag{2-12}$$

Equation (2-12) implies the lengthening of the Chandler period. Numerical analysis showed that the Chandler period is lengthened by about 29.8 days (DAHLEN, 1976 with correction by SMITH & DAHLEN, 1981).

Finally, we shall take the mantle anelasticity into account by assuming complex elastic moduli. Since κ is related to the Earth's elasticity through the static Love number k by

$$\kappa=ka^5\Omega^2/(3GA)$$

complex elastic moduli make κ complex as well as k. Hence, the Chandler angular frequency given by (2-12) also becomes complex.

$$\begin{aligned}\tilde{\sigma}_c&=\tilde{\sigma}_e-\sigma'\\&=(A/A_m)(e-\tilde{k}a^5\Omega^2/(3GA))\Omega-\sigma'\end{aligned} \tag{2-13}$$

where $\sim$ stands for a complex value.
The Chandler wobble Q_w is derived from the imaginary part of $\tilde{\sigma}_c$.

$$Q_w=-(A_m/A)(3GA/a^5\Omega^3)\sigma_c/(2\,\mathrm{Im}\,[\tilde{k}]) \tag{2-14}$$

$$\sigma_c=\mathrm{Re}\,[\tilde{\sigma}_c]\,.$$

§ 2. Solution to the basic wobble equations

The solution to the wobble equation (2-8) is most easily obtained in the frequency domain. A Fourier transform of (2-8) allowing for (2-11) and (2-13) yields

$$\begin{aligned}M(\sigma)&=\Phi(\sigma)/(\sigma-\tilde{\sigma}_c)\\\Phi(\sigma)&=(A_f/A)\phi_1(\sigma)-\phi_2(\sigma)\end{aligned} \tag{2-15}$$

If $\Phi(\sigma)$ has a white spectrum, Q_w can be estimated from the spectrum of $m(t)$ by

$$Q_w=\sigma_c/\Delta\sigma \tag{2-16}$$

where $\Delta\sigma$ is the full half width of $|M(\sigma)|^2$.

$$|M(\sigma_c\pm\Delta\sigma/2)|^2=|M(\sigma_c)|^2/2\,.$$

Random excitation of the Chandler wobble is not a bad approximation as shown by SEKIGUCHI (1976). Furthermore, the flatness of $\Phi(\sigma)$ just around σ_c is sufficient in order to estimate Q_w from (2-16). Most investigators so far have assumed the whiteness of Φ and presented estimates for Q_w. We will also take this view and estimate Q_w in Chapter 5.

3. Test of the variable Chandler period hypothesis

§ 1. The variable Chandler period hypothesis

Numerous authors suggested that the Chandler period is variable in time since the discovery of the Chandler wobble in the late 19-th century (CHANDLER, 1892; KIMURA, 1918; MELCHIOR, 1954, 1957; SEKIGUCHI, 1972, 1976; GAPOSCHKIN, 1972; CARTER, 1981). The hypothesis is characterized by the following empirical laws (MELCHIOR, 1957).

(1) The period of the Chandler wobble fluctuates. The maximum departure from the mean value is approximately 4%.

(2) Period and amplitude of the Chandler motion are proportional. The correlation coefficient is more than 0.8.

(3) A long Chandler period is correlated with a small amplitude of the annual motion.

If the Chandler motion is indeed variable, its intrinsic Q can never be estimated from the ratio of the spectral half width to the Chandler frequency. This is because the variable Chandler frequency inevitably broadens the width of the originally sharp line spectrum. Let the frequency be modulated by a fraction α. Ordinary harmonic analysis of this frequency-modulated time series is expected to yield a relatively broad peak in the frequency band of $f_c(1-\alpha)<f<f_c(1+\alpha)$ where f_c denotes the Chandler frequency. In this case, Q may be judged to be $Q_{app}=1/\alpha$. If α is 0.04 as suggested from the Melchior's first law, Q_{app} becomes 25, which has nothing to do with the intrinsic Q_w value.

The above argument makes the hypothesis very attractive, since it offers the explanation of an anomalously low Q of the wobble derived from the spectral analysis. However, the hypothesis has been suffering from serious defects, theoretically as well as observationally. The theoretical difficulty is that no physically plausible mechanism is presented which can cause the fluctuation of the Chandler period (NEWCOMB, 1892, MUNK & MACDONALD, 1960). Although a nonequilibrium pole tide is postulated as a possible cause, the theory still remains kinematical (DICKMAN, 1979; CARTER, 1981). From the observational point of view, it seems to us that the hypothesis is constructed on rather shaky grounds. In particular, the feasibility of the analyses indicating the variable period have not yet been fully tested. Hence, it is very probable that they may yield spurious "laws" described above even when they are applied to a synthetic polar motion with a invariant Chandler period and a finite Q_w.

We believe it is decisively important to test the observational "evidence" of the hypothesis at this stage because the mantle Q_m at the Chandler frequency is seriously affected by the reality of the variable

period. The above consideration leads us to testing the hypothesis by applying the same technique employed by the variable period hypothesis to synthetic polar motion. Tested are the following methods.

(1) Running Harmonic Analysis
(2) Revolution Angle Analysis
(3) Autocorrelation Approach
(4) Beat Period Analysis
(5) Running Maximum Entropy Spectral Analysis

The above methods represent most of the earlier analytical techniques although they may not be complete. If they do not reveal spurious time-variability for the invariant Chandler frequency model, they are considered to pass the test and vice versa. Before applying these methods, we shall describe in the next section how to generate synthetic polar motions.

§ 2. Generation of synthetic polar motion

As is well-known, the polar motion is composed of three parts. They are

(1) The Chandler wobble, the excitation mechanism of which is not yet resolved. The mean amplitude is about 0.″15.

(2) The annual wobble, which is most probably excited by seasonal change of atmospheric and hydrological effects (WILSON & HAUBRICH, 1976a). Its mean amplitude is 0.″10.

(3) Secular drift of the order of 0.″003/yr in the direction of 70°W.

In order to generate synthetic polar motion assuming an invariant frequency and a finite Q_w, excitation function Φ should be specified (see eq. (2-15)). Since the frequency component just around the Chandler frequency dominates the behavior of the excited wobble as seen from (2-15), purely random excitation is sufficient for the present purpose. The amplitude and phase of the excitation spectrum, $A(f)$ and $\theta(f)$, are defined as

$$A(f)=A_0=\text{const.}$$

$$\theta(f)=\text{uniformly random in the range of } 0\leqq\theta<2\pi\,.$$

The excitation spectrum $\Phi(f)$ is given by

$$\Phi(f)=A(f)\exp(i\cdot\theta(f))$$

$$=A_0\exp(i\cdot\theta(f))$$

A_0 should be taken as a scaling factor for the moment. The Fourier spectrum of the synthesized Chandler wobble is then computed from (2-15)

as

$$M(f)=\Phi(f)/(2\pi i(f-\tilde{f}_c))$$

$$\tilde{f}_c=\tilde{\sigma}_c/(2\pi)\,.$$

In practice, $M(f)$ and $\Phi(f)$ can be computed only at discrete frequencies f_k.

$$f_k=k\Delta f\,;\qquad k=0,1,\cdots,N-1\,.$$

The sampling interval Δf is related to the duration of the time series T by

$$\Delta f=1/T=1/(N\cdot\Delta t)$$

where Δt corresponds to the observational sampling interval and N is the number of observations.

A discrete inverse Fourier transform of $M(f_k)$ is carried out to produce a discrete time series of synthetic Chandler wobble, $\tilde{m}_c(t_k)$.

$$M_k=M(k\cdot\Delta f)$$

$$\tilde{m}_{c,j}=\tilde{m}_c(j\cdot\Delta t)=\sum_{k=0}^{N-1}M_k\cdot\exp(2\pi ik\Delta f\cdot j\Delta t)\,;\quad j=0,1,\cdots,N-1\,.$$

We set N to 2^{17} to utilize the Fast Fourier Transform (FFT). We take 1/12 and 1/20 year for Δt since actual polar motion is given at these intervals. Total length of the synthesized record, T, is either 10922 or 6553 year. Δf is thus less than 1.5×10^{-4} cpy (cycle per year). The ratio of the spectral half width Δf_h to the frequency interval Δf is calculated by

$$\Delta f_h/\Delta f=f_c/(Q_w\cdot\Delta f)\,.$$

The ratio is more than 5 even in the case of $Q_w=1000$ which seems to be the upper bound for the Chandler wobble Q. The above argument implies that the discrete time series thus generated does not significantly lose the original spectral character. Synthesized Chandler wobbles with various Q_w's are presented in Fig. 4 where mean amplitudes are scaled to 0.″15 by adjusting the factor A_0.

Synthesized wobble for each Q_w value shows characteristic beat phenomenon. If might seem queer at first sight that the single Chandler frequency model yields beat phenomenon characteristic of the multiple periods model. The finite Q_w, however, necessarily brings about beat and we will show the reason below.

We may roughly approximate the continuous Chandler wobble spectrum by a line spectrum composed of three spikes.

$$M(f)=A_0[\delta(f-f_c)+\delta(f+\Delta f_h-f_c)/2+\delta(f-\Delta f_h-f_c)/2]$$

where δ is the Dirac's delta function. We assume here that three com-

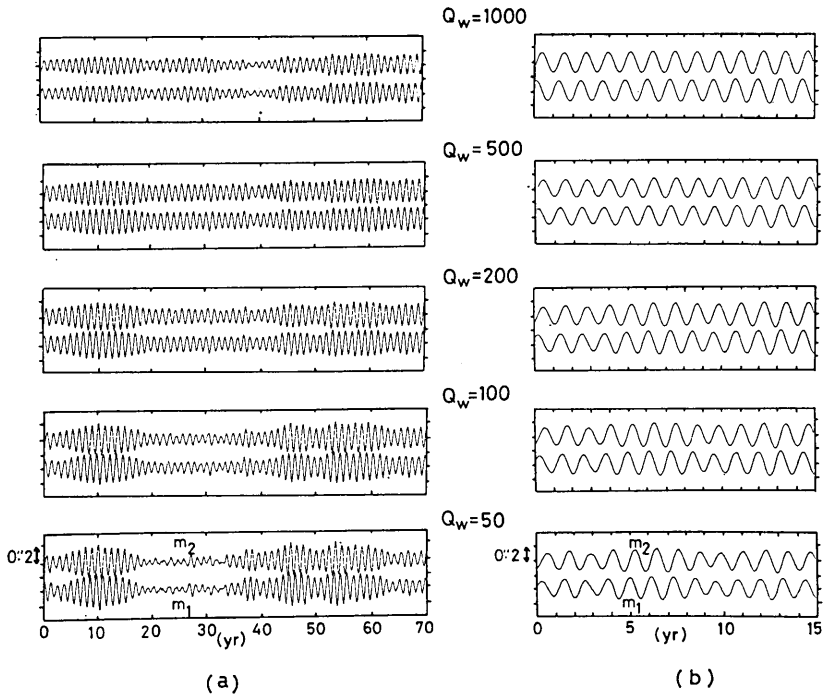

Fig. 4. Synthetic Chandler wobble of (a) ILS type (b) IPMS type.

ponents are in phase for simplicity.
Applying the inverse Fourier transform to the above expression and taking its real part, we obtain

$$m_1(t)=m_0[\cos(2\pi f_c t)+\cos(2\pi(f_c-\Delta f_h)t)/2+\cos(2\pi(f_c+\Delta f_h)t)/2]$$
$$=2m_0\cos^2(\pi\Delta f_h t)\cdot\cos(2\pi f_c t)\,.$$

Similar expression can be derived for m_2. It is obvious that m_1 and m_2 reveal beat phenomenon. The beat period, T_b, is given by

$$T_b=1/\Delta f_h=Q_w/f_c$$

Q_w value of 50 implies the beat period of about 60 years as observed in Fig. 4.

We generate synthetic polar motion by adding a stationary annual term of amplitude 0."1 and random observational noise with standard deviation of 0."03 or 0."01 to the synthesized Chandler wobble. The standard deviations of 0."03 and 0."01 correspond to the observational errors for ILS and IPMS/BIH data, respectively (YUMI, 1970; LAMBECK, 1980). We will call the synthetic data of sampling interval 1/12 year and observation noise 0."03 ILS-type. That data of sampling interval 1/20

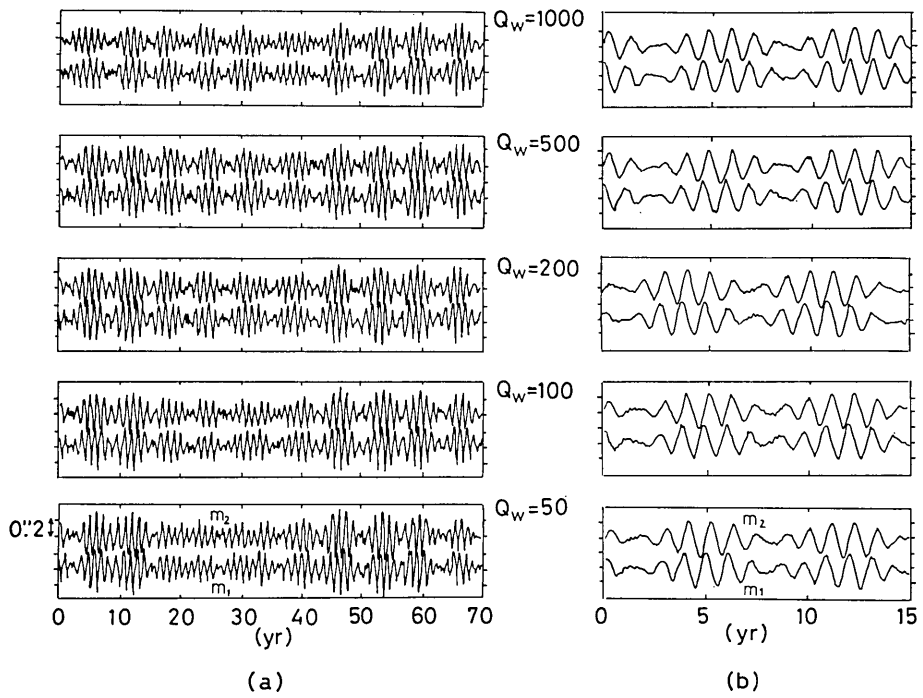

Fig. 5. Synthetic polar motion of (a) ILS type (b) IPMS type.

year and noise 0.″01 will be called IPMS-type hereafter (Fig. 5).

§ 3. Multiple period hypothesis

COLOMBO & SHAPIRO (1968) suggested the existence of two components of the Chandler period, each separated by about 10 days. Their argument is entirely based upon beat phenomenon observed in this century. Beat phenomenon in itself, however, can never be taken as evidence for multiple Chandler periods. As is shown by O'CONNELL & DZIEWONSKI (1976), wobble excited by large earthquakes for the model of single Chandler frequency and a finite Q_w does show beat phenomenon. We have already elucidated the reason completely in the preceding section.

COLOMBO & SHAPIRO speculated that the two component Chandler periods arise from mechanical interaction between the upper mantle and the remainder. However, recent theoretical investigation allowing for the low-Q layer in the upper mantle does not reveal the splitting of the Chandler frequency (SMITH & DAHLEN, 1981).

GAPOSCHKIN (1972) treated pole position data of 125 year duration and subjected the data to the spectral analysis. The spectrum showed the double-peak structure in the Chandler frequency band and he concluded the reality of two eigenperiods of the Chandler wobble (Fig. 6). The

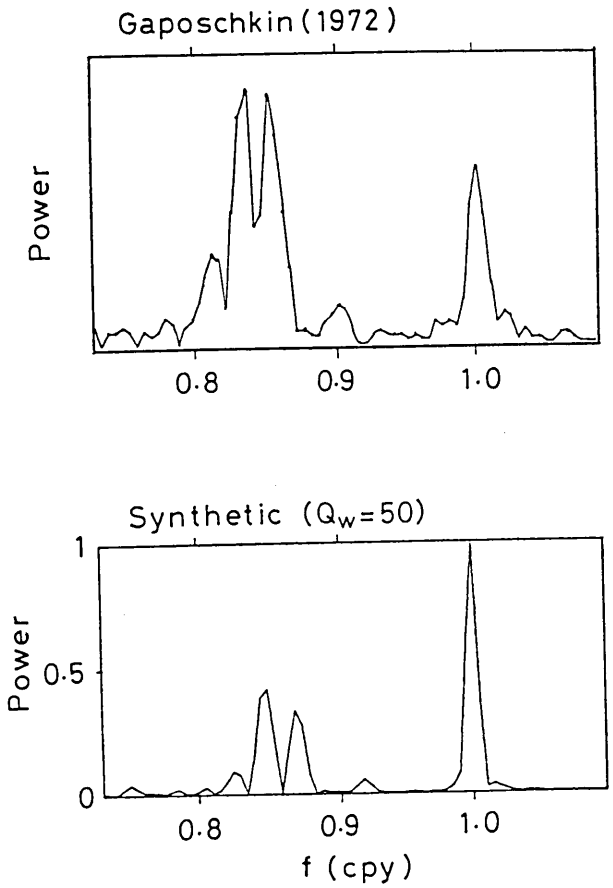

Fig. 6. Periodgram of the polar motion. (top) Gaposchkin's result (bottom) result for synthetic polar motion.

analytical procedure was as follows.

(1) Reduce observations into a discrete time series of a constant sampling interval (18 days).

(2) Apply a data window, w_j, to the discrete time series. w_j is defined as

$$w_j=(1-\cos(2\pi j/M))/2\,; \qquad j=0,1,\cdots,M-1$$

where M is the number of observations.

(3) Apply FFT to the windowed data and compute the power spectrum.

We synthesize polar motions of various Q_w values with a sampling interval of 18 days in the same way as described in the preceding section. M is set to 2600 (128 years). The result is shown in Fig. 6. The spectra

for $Q_w=50$ and 100 show the characteristic double-peak structure in the Chandler frequency band. The double-peak is most probably a product of the statistical fluctuation of the time series as discussed by PEDERSEN & ROCHESTER (1972). Thus the multiple-peak spectrum presented by GAPOSCHKIN cannot be regarded as significant.

The above arguments lead to the conclusion that there is no need at all to suppose multiple Chandler periods.

§ 4. Running Harmonic Analysis

If the Chandler frequency f_c varies in time while the seasonal excitation function remains constant, the magnitude of the excited annual wobble is expected to change due to the resonance effect. Let the excitation function be

$$\Phi_a=\tilde{A}\exp(2\pi i f_a t)\,.$$

Then, forced annual oscillation $\tilde{m}_a$ is derived from equation (2-15) as

$$\tilde{m}_a=\tilde{A}\exp(2\pi i f_a t)/(\tilde{f}_c-f_a)$$

where f_a denotes 1 cpy.

The closer the Chandler frequency approaches the annual frequency, the more the annual wobble would be excited. This is the Melchior's third law described in § 1.

MELCHIOR (1954, 1957) observed the expected relation between the annual wobble amplitude and the instantaneous Chandler frequency. The result is reproduced in Fig. 7a. He estimated the instantaneous frequency from ILS data for succesive intervals of one beat period (5~9 years). Since any frequency analysis (except for Maximum Entropy Method) from such short duration record should yield highly unstable results, Melchior's analysis is also likely to be affected by the stochastic fluctuation of the time series. Furthermore, Melchior's argument is based upon the assumption of a constant seasonal excitation function, which seems to us doubtful. In fact, the atmospheric excitation function calculated by WILSON & HAUBRICH (1976b) does show significant yearly variation.

We decided to test the feasibility of the Running Harmonic Analysis by applying it to the ILS-type synthetic data. We estimated the Chandler frequency and the annual components amplitude by the following scheme.

Preliminary annual components amplitude are calculated by

$$\tilde{m}^+=\sum\tilde{m}(t_k)\cdot\exp(-2\pi i f_a t_k)/N$$

$$\tilde{m}^-=\sum\tilde{m}(t_k)\cdot\exp(2\pi i f_a t_k)/N\,.$$

After removing these annual terms from the original data, we compute its Fourier transform.

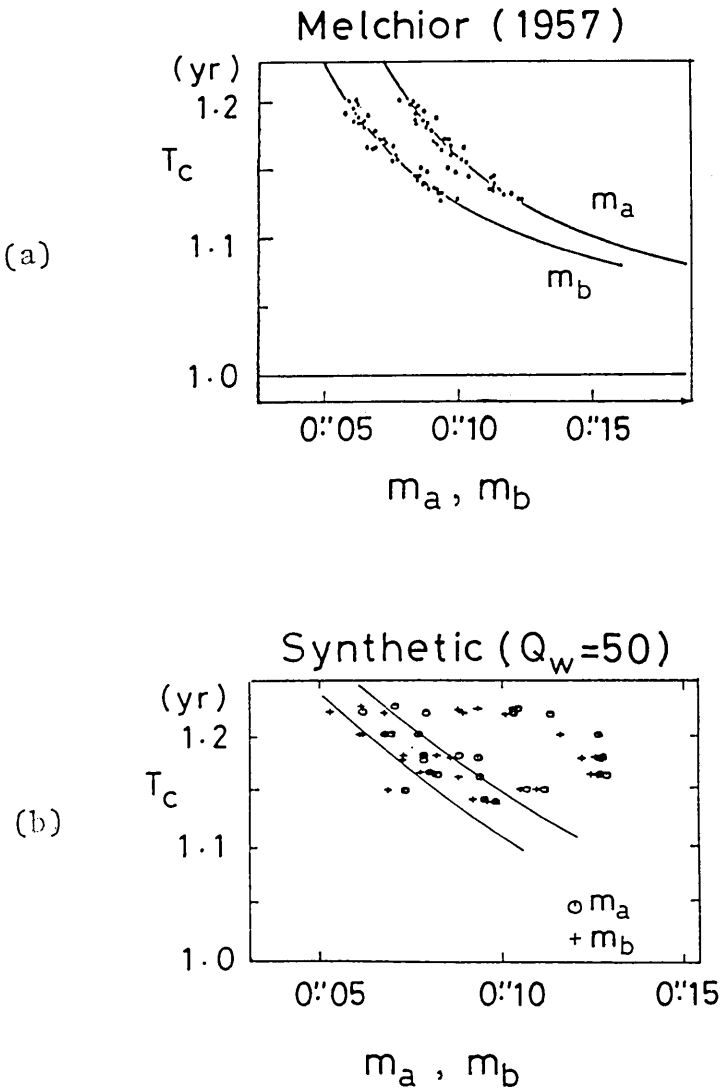

Fig. 7. Running Harmonic Analysis of the polar motion. m_a and m_b denote the lengths of semi-major and semi-minor axes of the annual ellipse. (a) after Melchior (1957) (b) result for ILS type synthetic polar motion.

$$\tilde{m}'(t_k)=\tilde{m}(t_k)-\tilde{m}^{+}\cdot\exp(2\pi i f_a t_k)-\tilde{m}^{-}\cdot\exp(-2\pi i f_a t_k)$$

$$M'(f)=\sum\tilde{m}'(t_k)\cdot\exp(-2\pi i f t_k)\,.$$

Searching for $\hat{f}_c$ which maximize $|M'(f)|^2$, we obtain an estimate for the Chandler frequency for the specific interval. $M'(f)$ is computed at every

0.001 cpy from 0.81 to 0.90 cpy. The Chandler amplitude $\tilde{m}_c$ is calculated by

$$\tilde{m}_c = \sum \tilde{m}'(t_k) \cdot \exp(-2\pi i \hat{f}_c t_k)/N .$$

Annual term amplitudes are recalculated from the time series $\tilde{m}''(t)$.

$$\tilde{m}''(t_k) = \tilde{m}(t_k) - \tilde{m}_c \exp(2\pi i \hat{f}_c t_k)$$

$$\tilde{m}^+ = \sum \tilde{m}''(t_k) \cdot \exp(-2\pi i f_a t_k)/N$$

$$\tilde{m}^- = \sum \tilde{m}''(t_k) \cdot \exp(2\pi i f_a t_k)/N .$$

Melchior regarded only results which satisfy the following commensurability as reliable.

$$T = T_c T_a/(T_c - T_a) \qquad (3\text{-}1)$$

where T denotes the duration of the analyzed interval. T_c and T_a are the Chandlerian and annual periods, respectively. We followed this criterion and only the results satisfying (3-1) within 1% error are adopted. The lengths of the major and the minor axes of the annual ellipse are presented together with the estimated Chandler period (Fig. 7b). The length of the semi-major axis is estimated to be $0.''10 \pm 0.''02$, fairly large fluctuation although data is originally synthesized from the constant annual amplitude model. The Chandler period also shows apparent scattering (1.13~1.22 years), although data is synthesized from a constant Chandler period model. The magnitudes of the fluctuations of the estimates for $(\tilde{m}^+, \tilde{m}^-)$ and T_c are comparable to those reported by MELCHIOR (Fig. 7). Hence, we may conclude that the fluctuation of the Chandler period and the annual term amplitude are more apparent than real.

We can see the apparent negative correlation between the annual term amplitude and the Chandler period in Fig. 7b (especially for the case $Q_w = 50$), although it is not so clear as observed in Fig. 7a. The third law of Melchior is thus explained by the constant Chandler period model.

§ 5. Revolution Angle Analysis

SEKIGUCHI (1976) proposed Revolution Angle Analysis to trace the temporal variation of the Chandler period. Let m_1^c and m_2^c be the Chandler components of m_1 and m_2, respectively. The revolution number, $R(t)$, is defined as

$$R(t) = \arctan(m_2^c(t)/m_1^c(t))/(2\pi) . \qquad (3\text{-}2)$$

The instantaneous Chandler frequency at time T_n is related to $R(t)$ by

$$f_c(T_n) = \frac{d}{dt} R(t)|_{t=T_n} .$$

In practice, $R(t)$ can be computed at only discrete time, t_j, at a sampling interval Δt. SEKIGUCHI approximated the discrete time series $R(t_j)$ for the succesive intervals of two years by a straight line

$$R(t_j) \sim a_n + f_c(T_n) \cdot t_j \,; \qquad T_n - (J-1)\Delta t \leqq t_j \leqq T_n + J\Delta t$$

a_n and $f_c(T_n)$ were determined by the least squares method. The standard deviation of the estimated $f_c(T_n)$ is calculated by

$$\kappa_n = (\sum_j \varepsilon_{nj}^2)^{1/2} \cdot [\sum_j \{(2J)t_j - (\Sigma t_j)\}^2]^{1/2} / \{D(2J-2)^{1/2}\}$$

where ε_{nj} and D are given by

$$\varepsilon_{nj} = R(t_j) - a_n - f_c(T_n)t_j$$

$$D = 2J\Sigma t_j^2 - (\Sigma t_j)^2 .$$

The fluctuation of the Chandler frequency thus determined is reproduced in Fig. 8a. He also computed a function F which corresponds to the probability density function of the Chandler frequency.

$$F(f) = \Sigma \exp[-(f - f_c(T_n))^2/(2\kappa_n^2)]/\kappa_n .$$

SEKIGUCHI reported the multiple-peak structure of F (Fig. 8b). He

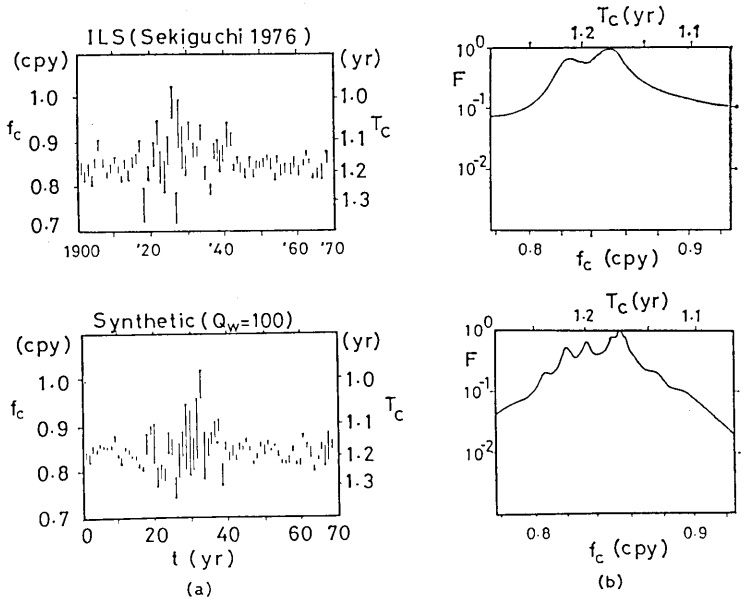

Fig. 8. (a) Temporal variation of the estimated Chandler frequency f_c by the Revolution Angle Analysis. (b) probability density function of the Chandler frequency f_c.

interpreted these results as evidence for the variable Chandler period.

The analysis appears convincing at first sight. There remains, however, a suspicion that the revolution number estimated by (3-2) may be severely distorted by the observational error, especially when the radius of the Chandler wobble diminished (around 1930s). Furthermore, there is a possibility that random excitation of the Chandler wobble may account for the characteristics discovered by SEKIGUCHI. Hence, it is natural to test the reliability of Revolution Angle Analysis by applying it to the synthesized polar motions described in § 2. Δt and J are set to 1/12 year and 12, respectively. The total number of sampling points is 840, corresponding to 70 years observation. The annual wobble, secular drift and observational error are excluded in this case. In order to definitely claim the variable Chandler period, Revolution Angle Analysis should yield a single fixed Chandler period when applied to the synthetic data.

The results are shown in Fig. 8. The apparent variation pattern of the estimated Chandler frequency is similar to that revealed by SEKIGUCHI, especially for $Q_w=100$. The probability density functions show multiple-peak structure for all Q values. The spacing of the peaks are from 0.01 to 0.02 cpy, comparable to that reported by SEKIGUCHI ($\Delta f=$ 0.025 cpy).

Since the Chandler wobble synthesized from the single period model is shown to yield the observational "evidence", there is no need to suppose the variable Chandler period. Although SEKIGUCHI's interpretation of Fig. 8 is not supported, the results will be found valuable in discussing the Chandler wobble Q in a later Chapter.

§ 6. Autocorrelation Approach

SEKIGUCHI (1972) related the autocorrelation of the Chandler wobble to the damping coefficient and the Chandler frequency, assuming the randomness of the excitation process.

$$C(\tau)\sim\exp(-\kappa\tau)\cdot[A\cos(2\pi f_c\tau)+B\sin(2\pi f_c\tau)] \qquad (3\text{-}3)$$

where κ and f_c denote the damping coefficient and the Chandler frequency. The autocorrelation, $C(\tau)$, is calculated at discrete points by

$$C(\tau=n\Delta t)=\sum[m_1^c(k\Delta t)m_1^c((k+n)\Delta t)+m_2^c(k\Delta t)m_2^c((k+n)\Delta t)]/(N-n)$$

where Δt and N are the sampling interval and the number of observations. The four parameters, $\{\kappa, f_c, A, B\}$, are determined to closely fit the expression (3-3), but the specific way is not described by SEKIGUCHI. We reproduce the results in Fig. 9 which shows fluctuating Chandler frequency. He also pointed out correlations between κ and $(2\pi f_c)$ and between κ and $C(0)$ (Fig. 9b, c). He interpreted these results as supporting evidence

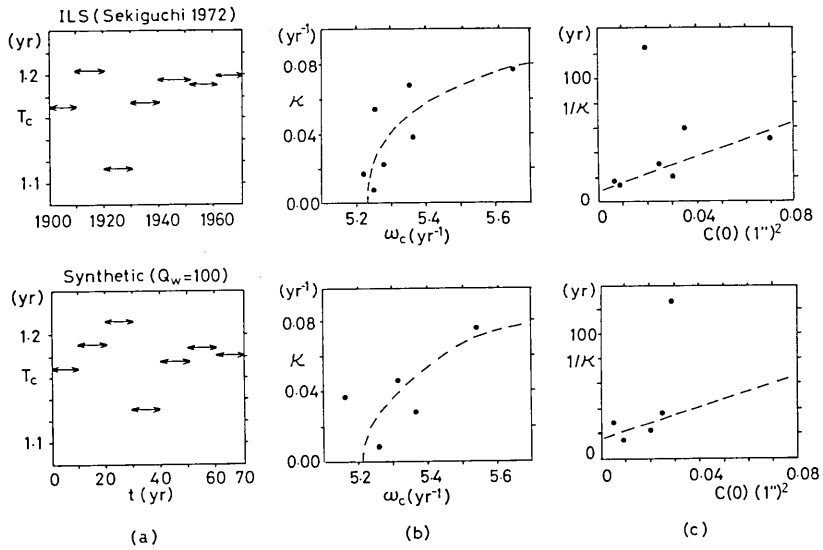

Fig. 9. (a) Variation of the Chandler period T_c estimated by the Autocorrelation approach. (b) Apparent correlation between the damping coefficient κ and the Chandlerian angular frequency ω_c. (c) Apparent correlation between the damping coefficient κ and the squared amplitude of the Chandler wobble $C(0)$.

for the time-variable Chandler period model proposed by him (SEKIGUCHI, 1961).

We apply the scheme after SEKIGUCHI to synthetic polar motions in order to test the fidelity of this approach. In practice, autocorrelations are calculated up to 30 lags ($\tau \leqq 2.5$ year) and we approximate them by (3-3). The sampling interval is 1/12 year. Synthetic wobbles do not include the annual term, secular drift or observational noise. The total number of observations is set at 840, corresponding to 70 years observation. We determine the four parameters so as to minimize the function defined as

$$F(\kappa, f_c, A, B) = \sum_{\tau} [C(\tau) - \exp(-\kappa\tau)\{A\cos(2\pi f_c\tau) + B\sin(2\pi f_c\tau)\}]^2$$

$$= \sum_{n} [C(n\Delta t) - \exp(-n\kappa\Delta t)\{A\cos(2\pi f_c n\Delta t) + B\sin(2\pi f_c n\Delta t)\}]^2 .$$

The estimation process for the unknowns becomes necessarily iterative on account of the nonlinearity of F. We adopt the POWELL's optimization procedure to find the most favorable values (POWELL, 1970). We present the results in Fig. 9. κ assumes negative values in some instances. However, the absolute values of the negative κ's are an order of magnitude

less than those of positive ones. Hence, we interpret negative κ's as implying virtually vanishing and neglect them in the following discussion.

The behavior of the fluctuations of κ and f_c closely resembles that found by SEKIGUCHI (Fig. 9a, b). We can also recognize apparent correlations between κ and f_c and between κ and $C(0)$ (Fig. 9b, c). The results described above imply that it is not necessary to suppose the variable Chandler period in order to explain the observed fluctuation of f_c and κ.

§ 7. Beat Period Analysis

CARTER (1981) suggested the time-variability of the Chandler wobble induced by the variable Chandlerian amplitude. His argument is based upon the fluctuation of the beat period of the polar motion. Beat phenomenon is induced from the closeness of the periods of the Chandlerian and the annual motions. The beat period is given by

$$T_b = T_c T_a / (T_c - T_a)$$

where T_c and T_a are the periods of the Chandlerian and the seasonal wobbles, respectively.

Inspection of the actual polar motion since 1900 reveals fluctuation of the beat period (Fig. 4). Carter interpreted the fluctuation as a product of the variable Cnandler period. He pointed out a correlation between the beat period and the mean magnitude of the polar motion, corresponding to the Melchior's second law. The result is reproduced in Fig. 10a.

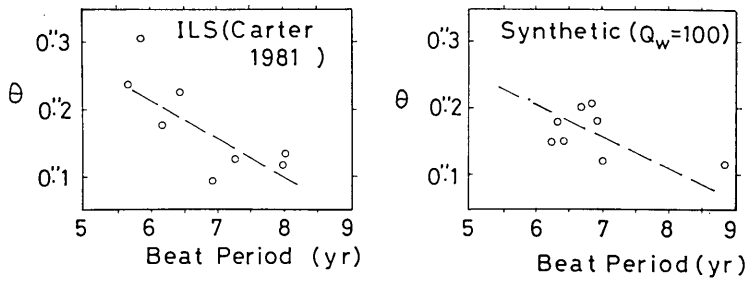

(a) (b)

Fig. 10. Apparent correlation between the beat period and mean magnitude of the polar motion.

The above analysis is, as Carter admitted, very simplistic and is based upon a questionable assumption that the magnitudes of the two kinds of wobble remain constant, at least within a cycle of beat phenomenon (5～

9 years). Since the amplitude of the atmospheric excitation fluctuates considerably year by year as shown by WILSON & HAUBRICH (1976b), the above assumption is inadequate. Even if the annual term amplitude remains constant, variation of the Chandler amplitude can cause the apparent fluctuation of the beat period. We will show it by examining the beat periods and the mean magnitude for the synthetic polar motions. The data is ILS-type of 70 years duration with the secular drift and observational noise excluded. This is a highly idealized situation. The result for $Q_w=100$ is presented in Fig. 10b. The apparent variations of the beat period and the mean magnitude are comparable to those reported by CARTER (Fig. 10a). Thus we can conclude that Beat Period Analysis has by no means the fidelity to contend the variable Chandler period.

§ 8. Running Maximum Entropy Specral Analysis

Burg's Maximum Entropy Method (MESA) has a high resolution and an ability to detect periodic components even from short duration records (less than one period) (ULRYCH & BISHOP, 1975). GRABER (1976) applied the technique to IPMS polar motion data for the overlapping intervals of 2.85 years each. He showed the apparent variations of the Chandler frequency and Q_w (Fig. 11). GRABER himself interpreted the results caused by a succession of sudden phase shifts, corresponding to random excitation. CARTER (1981) reinterpreted the result as supporting evidence for the time-variable Chandler frequency model. We will test below whether the

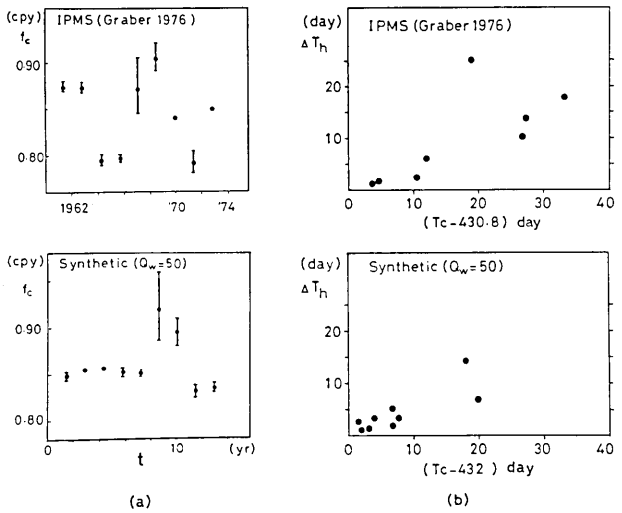

Fig. 11. (a) Time-variation of the Chandler frequency f_c estimated by Running MESA. (b) Apparent correlation between the departure from the mean period and full-half width period ΔT_h.

reinterpretation is adequate or not by applying GRABER's scheme to IPMS-type synthetic data. The procedure is as follows.

(1) Compute the prediction error filter of length 160 for the 15 years interval and extrapolate the data by predicting both in the forward and backward directions (SMYLIE, CLARKE & ULRYCH, 1973) until $2^{11}=2048$ points have been generated. Then apply the Fourier transform to the extended data and subtract the two annual components of frequencies 0.996 and 1.006 cpy from the original data.

(2) Divide the 15 years observation data into 9 overlapping segments of 2.85 years each. Then apply MESA to each interval to compute the instantaneous power spectrum. Since filter length is not specified by GRABER, we tried three cases for filter length L. Namely, $L=10$, 20 and 30.

The results is found to be insensitive to the choice of L. We show only the result for $L=20$ in Fig. 11a. The estimated Chandler frequency fluctuates considerably (± 0.03 cpy), comparable to the fluctuation reported by GRABER (± 0.05 cpy). It is interesting to note that the same correlation as presented by GRABER is found for the synthetic data between the departure from the mean frequency and Q (Fig. 11b). Furthermore, the fluctuation pattern of the estimated Chandler frequency resembles closely that given by GRABER (Fig. 11a).

The above observation indicates that the fluctuating Chandler frequency is likely to be more apparent than real. The variation is probably caused by random phase shifts as proposed by GRABER. There is no need to suppose the time-variable Chandler frequency from the results of Running Maximum Entropy Spectral Analysis.

4. Tracing of the instantaneous spectrum of the Chandler wobble

§ 1. Formulation of the instantaneous frequency analysis

We have shown in the preceding chapter that most of the earlier techniques are not qualified to claim to have detected observational evidence for the variable Chandler period. We shall present below a better and more reliable technique for tracing the spectral structure of a non-stationary time series.

The algorithm for tracing the time-varying spectrum of a real-valued time series is already derived by WIDROW & HOFF (1960) and reviewed by GRIFFITHS (1975). Since the polar motion is conveniently expressed in a complex form, we derive below an algorithm extended for a complex-valued time series.

A discrete stationary time series, X, can be deconvolved into a white noise such that

$$\sum_m h_m \cdot X(k-m)=w(k) \tag{4-1}$$

where h_m denotes a prediction error filter coefficient and w is a white noise with zero mean.
A non-stationary time series, Y, is expressed in the same form as (4-1) if we allow for the temporal variation of the prediction error filter.

$$\sum_m g_m(k) \cdot Y(k-m)=w(k)\,. \tag{4-2}$$

The local prediction error filter at time k, $\{g_m(k),\ m=0\sim M\}$, is determined so as to minimize the variance of the noise. The variance of w at time k is defined as

$$V_k(g_1, g_2, \cdots, g_M)=E[|\sum_m g_m(k) \cdot Y(k-m)|^2]$$

where E does not imply a time average but an ensemble average. $g_0(k)$ is fixed to unity without loss of generality. Note that V_k is not analytical with respect to $g_m(k)$. However, the "gradient" of V_k with respect to $g_m(k)$ is constructed by the formal differentiation of V_k with respect to the complex conjugate of $g_m(k)$.

$$\frac{\partial V_k}{\partial g_m{}^*}=2E[\,Y^*(k-m) \cdot \sum_n g_n(k)\,Y(k-n)]$$

$$\sim\ 2\,Y^*(k-m) \cdot \sum_n g_n(k)\,Y(k-n)$$

where * designates complex conjugate.
Starting with an initial guess, $g_m{}^0(k)$, we can obtain $g_m{}^+(k)$, an improved estimate for $g_m(k)$, by the steepest descent procedure.

$$g_m{}^+(k)=g_m{}^0(k)-2\mu\,Y^*(k-m) \cdot \sum_n g_n{}^0(k) \cdot Y(k-n)$$

where

$$\mu=\alpha/(M \cdot C)$$

$$C=E[|\,Y(k)-E[\,Y(k)]|^2]$$

$$0<\alpha<1\,.$$

When non-stationarity is relatively weak and the filter coefficients remain nearly constant within the characteristic time of the stochastic process, $g_m(k-1)$ may be substituted for $g_m{}^0(k)$ in the above expression. Then we obtain

$$g_m(k)=g_m(k-1)-2\mu\,Y^*(k-m) \cdot \sum_n g_n(k-1)\,Y(k-n)\,. \tag{4-3}$$

We may replace the ensemble average operation for the computation of C by time averaging in this case because a rough estimate is sufficient for the determination of μ. If α lies in the range 0.0–1.0, it can be proved by an analogous scheme to GRIFFITHS's (1975) that the successive updating by (4-3) yields the desired filter after some transient time. Noticing the whiteness of $w(k)$ in (4-2), the relative instantaneous power spectrum at time k is computed by

$$P(f\,;\,k)=1/|\sum_n g_n(k)\cdot\exp(2\pi i f n\Delta t)|^2 \qquad (4\text{-}4)$$

where Δt is the sampling interval.

Numerical examples are presented below to show the excellent performance of this method.

(1) Sinusoidally frequency-modulated Chandler wobble

Synthetic sample data, $z(t)$, is constructed by the following formula (Fig. 12a, b).

$$\frac{dz}{dt}=2\pi i F(t)\cdot z$$

$$F(t)=\hat{f}_c(1+A\sin(2\pi t/T_m))$$

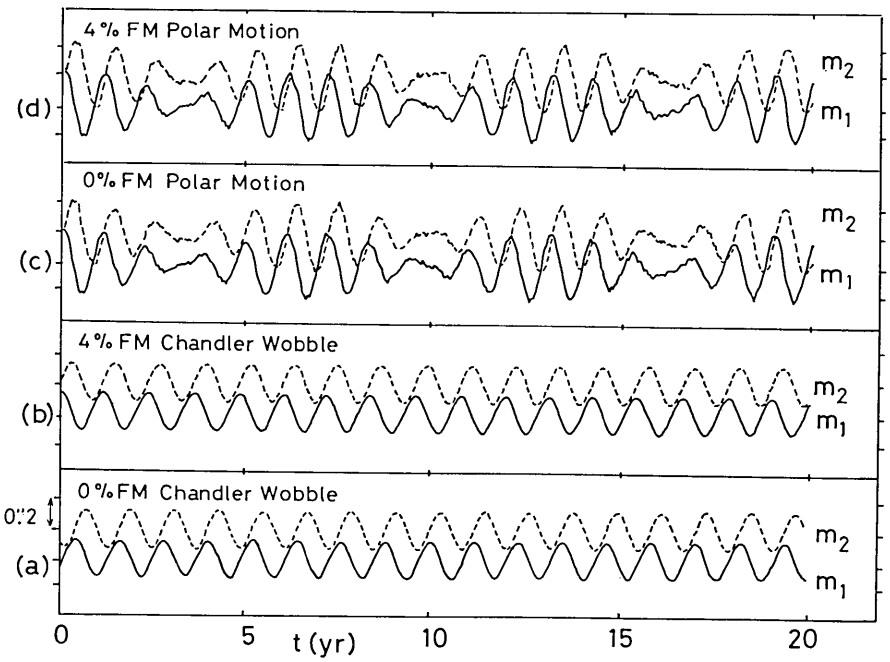

Fig. 12. (a) (b) Synthetic frequency-modulated Chandler wobble. (c) (d) Synthetic frequency-modulated polar motion.

$$z(t)=0.''15\cdot\exp\left(2\pi i\int F(t)dt\right)$$

where $F(t)$ is the instantaneous frequency with a mean value of $\hat{f}_c=0.845$ cpy. The modulation factor A is set to either 0 or 0.04 and the modulation period T_m is 6.45 years as suggested by CARTER (1981). The sampling interval is 0.05 year and the number of data points is 360, corresponding to IPMS/BIH data (Fig. 12a, b). Before the application of the instantaneous frequency analysis, we must specify three parameters in advance. They are the initial guess for $\{g_m(k)\,;\ m=1, 2, \cdots, M-1\}$, filter length M and the convergence factor α. It has been found from our experience of group velocity analysis of seismic surface wave by this method that M should be as long as the characteristic time of the data (OKUBO & TSUBOI, 1982). The characteristic time in this case is the Chandler

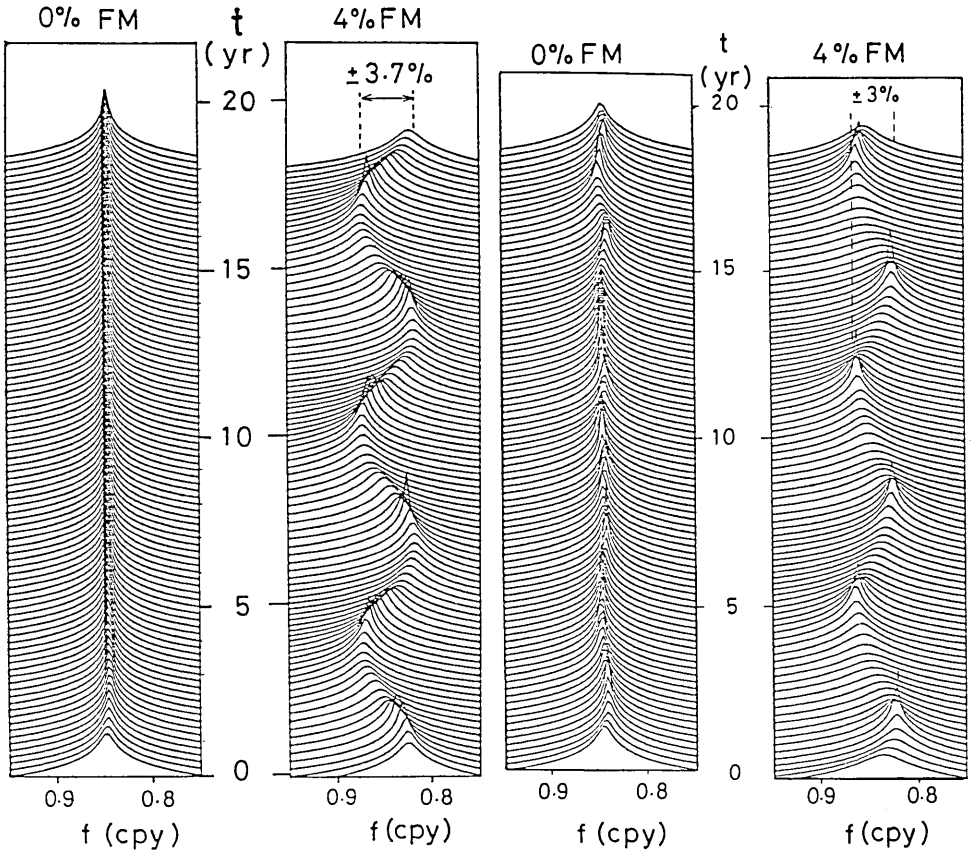

Fig. 13. Evolution of the instantaneous power spectrum of data given in Fig. 12 a, b.

Fig. 14. Evolution of the instantaneous power spectrum of data given in Fig. 12 c, d.

period of about 1.2 years, implying $M \gtrsim 25$. We take $M=30$ (1.5 years) as the filter length. The initial guess for the prediction error filter is obtained from the preliminary application of this method to the backward extrapolated time series of 150 data points. The initial guess for the preliminary analysis is $g_m^0(1)=\delta_{m0}$, where δ is the Kronecker's delta. There is no objective criterion for determining α. After several trials and errors, we find $\alpha=0.2$ gives the most favorable result (Fig. 13). We see from Fig. 13 that the technique does not yield spurious fluctuation of the instantaneous frequency for the unmodulated data. The result for the 4% frequency-modulated data reveals expected magnitudes both for A and T_m. The excellence of the performance of this method is thus clearly exhibited.

(2) Frequency-modulated Chandler wobble together with the annual term and observational noise.

In practice, it is impossible to directly observe the Chandler wobble. Observed polar motion is in the form of

$$u(t)=z(t)+0.''1 \exp(2\pi i f_a t)+w(t)$$

where f_a denotes 1 cpy and $w(t)$ is the white noise with a standard deviation of 0.″01, corresponding to IPMS/BIH observation (Fig. 12c, d). Since we are interested in the variation of $F(t)$, removal of the annual component is desirable to enhance the performance of this method. For this purpose, we apply a recursive low-pass filter with a cutoff frequency of 1/380 day^{-1} (SAITO, 1978). In order to reduce the end effect of the recursive filtering, we extrapolate the original data until 1000 points have been generated. The low-pass filter is applied to the extended data first in the forward direction of the time axis, next in the backward direction to compensate the phase shift induced by the forward filtering. The result of the instantaneous frequency analysis to the filtered data is given in Fig. 14. Although a slight fluctuation of the estimated instantaneous frequency is observed for the unmodulated data, we can judge the fluctuation insignificant without difficulty. The results for the 4% frequency-modulated data are almost the same as the results of (1), except for the slight diminution of the estimated modulation factor A.

The above observation ensures the method's detecting power of the variable Chandler period from the actual data if it really exists at all.

(3) Confidence interval

The instantaneous frequency analysis of the randomly excited polar motion is useful in estimating the confidence interval of the detected fluctuation of the period. We apply the technique to IPMS-type synthetic polar motions after the preprocessing described in (2). The parameters needed in the analysis are determined in the same manner as in (2). The

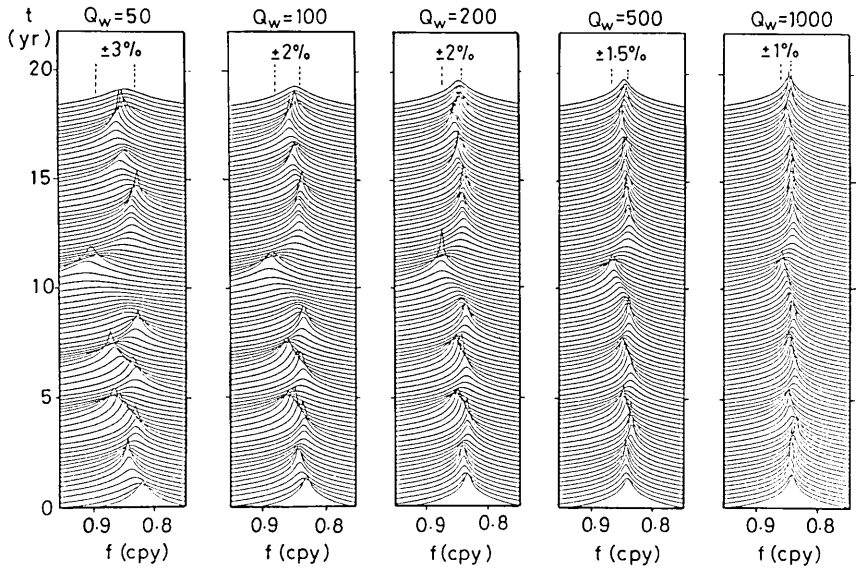

Fig. 15. Instantaneous power spectra for the time-invariant Chandler period model.

results are presented in Fig. 15. We observe a $\pm 1 \sim 2\%$ fluctuation of the instantaneous frequency from Fig. 15, although the data was synthesized from constant Chandler period models. Hence, we should not regard a $\pm 1 \sim 2\%$ change in the instantaneous frequency as significant.

One may argue from the results that the instantaneous frequency analysis does not yield reasonable estimates because we obtain fluctuating instantaneous frequency from the time-invariant period models. The criticism, however, is inadequate since the apparent instantaneous frequency does fluctuate due to the random excitation.

§ 2. Instantaneous Frequency Analysis of IPMS and BIH data

Two data sets on the polar motion from 1962.0 to 1980.0 are subjected to the Instantaneous Frequency Analysis. Internatihnal Polar Motion Service (IPMS) publishes the pole positions referred to the Conventional International Origin since 1962.0 (YUMI, 1980). The sampling interval is 0.05 year. The Bureau International de l'Heure (BIH) also deduces pole path since late 1955. The BIH adopted a "mean pole of epoch" as origin until 1968.0. The results since 1962.0 were reduced to the CIO reference by the BIH. We use the "BIH Global Solution" with a minor correction to conform to the 1979 BIH system (BIH, 1979). The sampling interval is 0.05 year.

We remove the annual term from the polar motion in the same way as described in (2) of § 1. The instantaneous frequencies from 1963.55 to

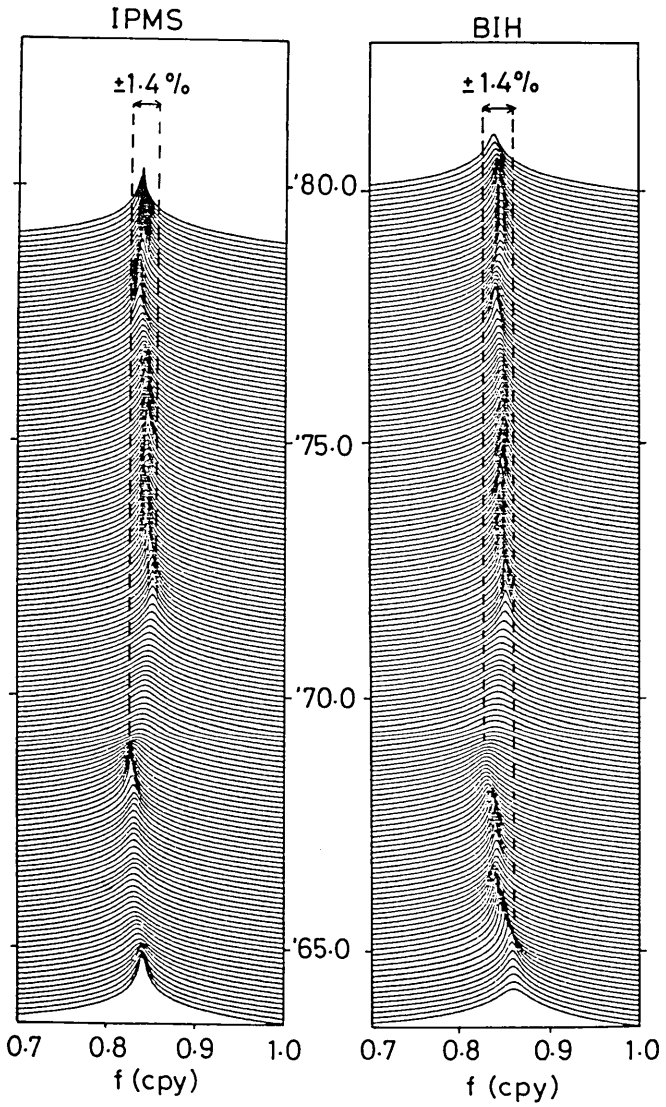

Fig. 16. Evolution of the instantaneous power spectrum for IPMS and BIH data.

1980 are shown in Fig. 16. The variation patterns of the instantaneous Chandler frequency from the two data sets are similar to each other in spite of the difference of the data reduction processes by the two agencies. The maximum departure of the instantaneous Chandler frequency is $\pm 1.4\%$, much smaller than those suggested by Carter for IPMS data ($\pm 7\%$) and by Melchior for ILS data ($\pm 4\%$). The fluctuation of the Chandler frequency can be judged to be insignificant since the significance

level of the variable Chandler frequency is about $\pm 1 \sim 2\%$ ($Q \geqq 100$) as shown in the preceding section. Thus we cannot find supporting evidence for the variable Chandler period from either IPMS or BIH data.

We applied the Instantaneous Frequency Analysis to ILS data of much longer record than IPMS and BIH. The results since 1963.55 are quite different from those obtained from IPMS and BIH data, most probably due to the higher noise level. Hence, we abandoned the idea of subjecting the earlier polar motion data of ILS to the Instantaneous Frequency Analysis.

5. Estimation of the Chandler wobble $Q(Q_w)$

§ 1. Difficulties in estimating Q_w by the spectral analyses.

Now that most of the observational evidence for the variable Chandler period is found to be doubtful and since it is also explained by the constant Chandler period model, we will proceed to estimate Q_w by assuming a time-invariant Chandler period. Q_w is most easily derived from the spectral half width using equation (2-16). There are three kinds of spectral analyses. We will discuss below the fundamental difficulties for each of them when applied to actual data in order to estimate Q_w.

(1) Periodgram approach

The Fast Fourier Transform makes this method attractive, especially when we have to handle a large quantity of data. However, the frequency resolution of the resultant spectrum is limited to the inverse of the total duration of the time series. Since the power spectrum estimated by this method is, in general, very ragged, we must smooth it by applying a suitable window to enhance the statistical stability. Hence, the sharp line spectrum as that of the polar motion will be inevitably blurred at the expence of the increased reliability (PEDERSEN & ROCHESTER, 1972). Furthermore, O'CONNELL and DZIEWONSKI (1976) showed that the periodgram yields an apparent $Q_{app}=100$ even when it is applied to synthetic polar motion with an intrinsic $Q_w=10000$. The above argument implies that the periodgram approach gives only the lower bound for Q_w.

(2) Blackman-Tukey's method

This technique suffers from the same difficulty as that of periodgram. Power spectrum is estimated from the Fourier transform of the autocorrelation of the time series, followed by a smoothing by some spectral window (BLACKMAN & TUKEY, 1958). The detail of the spectral structure around the sharp peak is inevitably blurred. So we must keep in mind that the method also gives only a lower bound for Q_w.

(3) Burg's Maximum Entropy Spectral Analysis (MESA)

This technique is clearly superior to the conventional methods (Periodgram and Autocorrelation approaches) in detecting periodic components BURG, 1967, 1968; LACOSS, 1971). MESA is shown to be efficient for analyzing a short duration record (ULRYCH, 1972).

As is well-known, the most serious defect of MESA is the lack of an objective criterion for determining the optimum length of the prediction error filter. Although a general criterion called FPE is proposed (AKAIKE, 1969, 1970; ULRYCH & BISHOP, 1975), it does not always work well. In fact, FPE criterion fails to yield the annual peak in the polar motion spectrum of 15 years duration (GRABER, 1976). Until a reasonable criterion is found, estimates of Q_w from MESA should not be trusted.

In order to find a reliable estimate of Q_w, we proceed as follows.

(1) Apply MESA to the synthesized polar motions of various Q_w's described in Chapter 3 and observe the variation of the apparent Q_{app} as a function of the filter length L.

(2) Apply MESA to the actual polar motion and compute Q_{app} for various L's.

(3) Compare the results from (1) and (2) and find the intrinsic Q_w.

The above procedure may appear too simplistic and naive at first, but we believe it is the most efficient and statistically reliable method for estimating Q_w. In other words, the above method (hereafter called simulation approach) refines the first approximation of the polar motion spectrum parameters derived by previous investigations (f_c=0.85 cpy and Q_w=10$\sim$1000).

Since MESA is the nonlinear estimation technique, the resultant spectrum is expected to depend on several factors such as the sampling interval, total observation duration, observational noise magnitude and so on. We will apply MESA to the actual data and synthetic data corresponding to those analyzed by CURRIE (1974) and by GRABER (1976).

§ 2. Analysis of ILS data

CURRIE (1974) applied MESA to ILS data of 70 years observation. He determined the filter length empirically so that the spectrum does not show highly ragged features. He averaged several estimates for Q_w obtained from various filter lengths. The above procedure is *ad hoc* and averaging lends no support for the adequacy of the estimated Q_w.

We investigate the variation of the apparent Q_{app} as a function of the filter length L. The behavior of $Q_{app}(L)$ is quite complex and is very sensitive to L (Fig. 17a). Calculated $Q_{app}(L)$ for the actual ILS data shows similar feature to those for the synthetic data (Fig. 17a). The above observation suggests that the variation pattern of $Q_{app}(L)$ is indeed

useful for the identification of the intrinsic Q_w value. We find from Fig. 17 that the curves of $Q_{app}(L)$ of natural $Q_w=50\sim100$ well fit the observed variation pattern of $Q_{app}(L)$ for the actual ILS data.

As was discussed in § 8 of Chapter 3, removal of the annual term from the observation is expected to improve the estmimation of Q_w. We extrapolate the time series with a prediction filter of $L=50$ until $2^{12}=4096$ points have been generated. Then we apply the Fourier transform to the extended data and subtract annual components of frequencies between $0.993\leqq f\leqq1.005$ cpy from the original data. We apply MESA to this preprocessed data. The results are presented in Fig. 17b. As is expected, fluctuation of $Q_{app}(L)$ diminishes compared with the raw analysis (Fig. 17a). Comparing the behavior of $Q_{app}(L)$ for the actual data with those for the synthetic data of various intrinsic Q_w's, we arrive at the conclusion that $50\lesssim Q_w\lesssim100$ is the most probable estimate for ILS data.

§ 3. Analysis of IPMS data

GRABER (1976) contended $Q_w=600$ from the MESA spectrum of IPMS data of 15 years duration. The value is significantly larger than that obtained in the preceding section. The difference in the two data sets are

(1) sampling interval
(2) total observation length
(3) magnitude of observational noise

We think (2) is the principal cause of the widely different estimates of Q_w from ILS and IPMS data. Recall the time-domain feature of the synthesized polar motions with various natural Q_w's (Figs. 4b, 5b). Note the visual similarity of the time-domain features between the synthetic Chandler wobbles of various Q_w's (Fig. 4b). As was discussed in § 3 of Chapter 3, more than 50 years data is required to observe the effect of Q_w in time domain.

GRABER assumed that the optimum filter length corresponds to 53% of the total observation period. The adopted filter length is $L=160$ while the total number of observations is 298. The filter length seems to us much longer than the optimum length. In order to test whether the filter length used by GRABER is adequate or not, we apply MESA after GRABER to IPMS-type data. The data is preprocessed as described in § 7 (1) of Chapter 3. The behavior of the calculated Q_{app} for the syntheitic data of various natural Q_w's is compared with that for the actual data as a function of the filter length L (Fig. 17c). We find in Fig. 17c that Q_{app} exceeds Q_w over a wide range of L. In particular, $Q_{app}(L=160)$ is 2 to 10 times larger than the intrinsic Q_w. One may argue that $Q_{app}(L=160)$ happens to be equal to the natural Q_w when $Q_w=500$. The behavior of $Q_{app}(L)$ of $Q_w=500$, however, clearly differs from that reported by GRABER

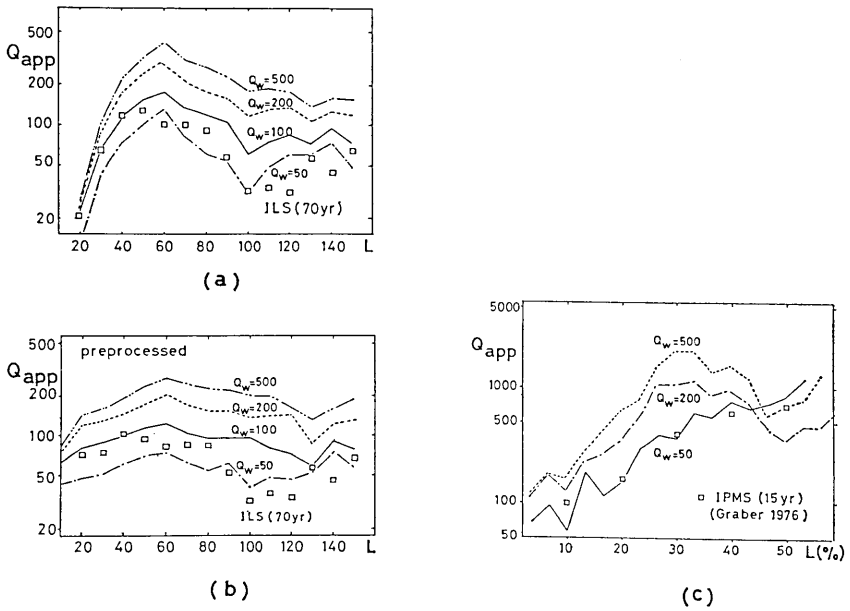

Fig. 17. Apparent Q derived by MESA as a function of filter length L. (a) □ designates the Q_{app} of ILS data. (b) result from the preprocessed data. (c) result for preprocessed IPMS and IPMS-type data. □ designates the result from GRABER (1976).

(Fig. 17c). On the other hand, we see that $Q_{app}(L)$ of natural $Q_w=50$ well fits the variation pattern of $Q_{app}(L)$ for the actual data. Hence, we may conclude that the intrinsic Q_w lies between 50 and 100 from the above discussions. GRABER's estimate of $Q_w=600$ is most likely to be due to his inappropriate choice of L.

6. Effects of the mantle anelasticity upon the Chandler wobble

§ 1. Theoretical calculation of Q_w

We present below a theory which is the extension of the theory for the perfectly elastic Earth by SASAO, OKUBO & SAITO (1980). As is discussed in Chapter 2, the Chandlerian angular frequency for the elastic, oceanless Earth is given by

$$\sigma_e=(A/A_m)(e-\kappa)\Omega$$

$$\kappa=ka^5\Omega^2/(3GA)\,.$$

Anelasticity of the mantle is expressed by complex elastic moduli, $\tilde{K}$ and $\tilde{\mu}$. The bulk and shear Q's are given by

$$Q_K^{-1}=\mathrm{Im}\,[\tilde{K}]/\mathrm{Re}\,[\tilde{K}]$$

$$Q_\mu^{-1}=\mathrm{Im}\,[\tilde{\mu}]/\mathrm{Re}\,[\tilde{\mu}]\,.$$

Complex elastic moduli lead to complex $\tilde{k}$ and $\tilde{\kappa}$. The resultant complex Chandler angular frequency allowing for the equilibrium pole tide is given by

$$\begin{aligned}\tilde{\sigma}_c&=(A/A_m)(e-\tilde{\kappa})\Omega-\sigma\\&=\sigma_c(1+i/(2Q_w))\end{aligned}\qquad(2\text{-}13)$$

where

$$\sigma_c=\sigma_e-\sigma'$$

$$Q_w=-(A_m/A)(3GA/a^5\Omega^3)\sigma_c/(2\,\mathrm{Im}\,[\tilde{k}])\,.\qquad(2\text{-}14)$$

We utilize Rayleigh's principle in order to calculate the imaginary part of $\tilde{k}$, arising from the small imaginary elastic moduli. Variational form for the tidal deformation of the Earth is similar to that for the free oscillation (TAKEUCHI & SAITO, 1972). The only difference between the two is the treatment of the boundary condition and the angular frequency. It is described by using the y-notation after TAKEUCHI & SAITO as

$$\begin{aligned}&a^2[y_1y_2+n(n+1)y_3y_4+(4\pi G)^{-1}y_5y_6]_{r=a}=\int F(y_j,\dot{y}_j,p_i)dr\\&F(y_j,\dot{y}_j,p_i)=(\lambda+2\mu)r^2\dot{y}_1^2+2\lambda r\dot{y}_1Y+(\lambda+\mu)Y^2\\&\quad+n(n+1)ry_4(r\dot{y}_3+y_1-y_3)+n(n^2-1)(n+2)\mu y_3^2\\&\quad+2(n+1)\rho ry_1y_5-2n(n+1)\rho ry_3y_5\\&\quad-2\rho gry_1Y+(4\pi G)^{-1}r^2y_6^2\,;\qquad(6\text{-}1)\\&\qquad j=1,3,5:\ i=1,2\end{aligned}$$

where

$$Y=2y_1-n(n+1)y_3$$

$$\lambda=K-(2/3)\mu$$

$$p_1=K\,,\quad p_2=\mu$$

$(\dot{\ })$ designates d/dr. n is the degree of spherical harmonic and it is 2 in this case.

Let the perturbation of p_i and the resultant variations of y_j and $\dot{y}_j$ be δp_i, δy_j and $\delta\dot{y}_j$, respectively. Variation of (6-1) is

$$\begin{aligned}&a^2[y_1\delta y_2+y_2\delta y_1+n(n+1)(y_3\delta y_4+y_4\delta y_3)+(4\pi G)^{-1}(y_5\delta y_6+y_6\delta y_5)]_a\\&=\int\frac{\delta F}{\delta p_i}\delta p_i dr+\int\left[\frac{\delta F}{\delta y_j}-\frac{d}{dr}\left(\frac{\delta F}{\delta\dot{y}_j}\right)\right]\delta y_j dr-\frac{\delta F}{\delta\dot{y}_j}\delta y_j\Big|_0^a.\end{aligned}\qquad(6\text{-}2)$$

Since $y_2(a)=y_4(a)=\delta y_2(a)=\delta y_4(a)=\delta y_6(a)=0$ and $y_6(a)=(2n+1)/a$ when y_j is the response to the unit external potential, the left hand side of (6-2) reduces to

$$LHS=a(4\pi G)^{-1}(2n+1)\cdot\delta y_5(a)\,. \tag{6-3}$$

The integrand of the second term on the right hand side of (6-2) vanishes since the term in the bracket is the Euler equation itself. The third terms are given by

$$\begin{aligned}\frac{\delta F}{\delta \dot{y}_1}&=2r^2y_2\\ \frac{\delta F}{\delta \dot{y}_3}&=2n(n+1)r^2y_4\\ \frac{\delta F}{\delta \dot{y}_5}&=2(4\pi G)^{-1}r^2y_6\,.\end{aligned} \tag{6-4}$$

Substituting (6-3) and (6-4) into (6-2) yields

$$\delta y_5(a)=-\frac{4\pi G}{(2n+1)a}\cdot\int\frac{\delta F}{\delta p_i}\delta p_i dr\,. \tag{6-5}$$

Since Love number k is given by $y_5(a)-1$, we obtain the variation of k from (6-5) by

$$\delta k=-\frac{4\pi G}{(2n+1)a}\cdot\int\frac{\delta F}{\delta p_i}\delta p_i dr \tag{6-6}$$

$$\delta p_1(r)=\delta K(r)=iQ_K^{-1}K(r)$$

$$\delta p_2(r)=\delta\mu(r)=iQ_\mu^{-1}\mu(r)\,.$$

Since Q_K is supposed to be several orders of magnitude larger than Q_μ in most Earth models, we will neglect Q_K and investigate the effect of Q_μ alone.

$$\begin{aligned}\frac{\delta F}{\delta\mu}=&(4/3)[ry_2-3KY/2]^2/(\lambda+2\mu)^2+n(n+1)(ry_4/\mu)^2\\ &+n(n^2-1)(n+2)y_3^2\,.\end{aligned} \tag{6-7}$$

(6-6) and (6-7) give the desired imaginary part of the Love number $\tilde{k}$. We present the Fréchet kernel in Fig. 18 for the model 1066A (GILBERT & DZIEWONSKI, 1975) and the isotropic PREM (DZIEWONSKI & ANDERSON, 1981). Surface ocean layers in the model PREM are replaced by solid layers of small shear velocity ($V_s=0.1$ km/sec). We assume Q_μ to be infinite except in the mantle and it is not a bad approximation since the Chandler wobble is almost free from the inner core motion. Calculated Q_w's are presented in Table 3 as $Q_w^{(0)}$, the expected Q_w when the mantle Q_m is independent of frequency. $Q_w^{(0)}$ is about 1.5 times larger

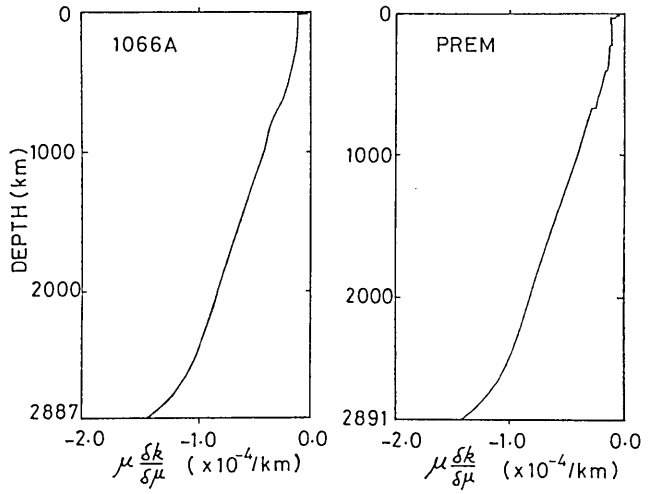

Fig. 18. Fréchet kernel of the Love number k for the two Earth models.

Table 3. Theoretical parameters of the Chandler wobble.

	1066A	PREM
Lower mantle Q at 200 sec	400	312
$Q_w^{(0)}$	573	481
Chandler period for		
: anelastic, oceanless Earth	408.9 ∿ 412.8 days	409.6 ∿ 413.7 days
: anelastic Earth with oceans	438.7 ∿ 442.6 days	439.4 ∿ 443.5 days

$Q_w^{(0)}$ designates theoretical Q_w for the frequency-independent Q_m model.

than the lower mantle Q_m.

If Q_m depends on frequency in the form of

$$Q_m(\sigma) = Q_m(\sigma_0) \cdot (\sigma/\sigma_0)^\alpha ,$$

then Q_w is expected to be modified from $Q_w^{(0)}$ to

$$Q_w = Q_w^{(0)} \cdot (\sigma_c/\sigma_0)^\alpha .$$

The frequency dependence exponent α is given by

$$\alpha = \ln (Q_w/Q_w^{(0)}) / \ln (\sigma_c/\sigma_0) . \qquad (6\text{-}8)$$

We have discussed the observed Q_w in Chapter 5 and the result is

$$50 \lesssim Q_w \lesssim 100 . \tag{6-9}$$

Combination of (6-8) and (6-9) yields

$$\ln (50/Q_w^{(0)}) \lesssim \alpha \ln (\sigma_c/\sigma_0) \lesssim \ln (100/Q_w^{(0)}) . \tag{6-10}$$

Substituting $Q_w^{(0)}$'s from Table 3, $2\pi/\sigma_c=435$ sidereal days and $2\pi/\sigma_0=200$ sec into (6-10), we obtain

$$0.143 < \alpha < 0.201 \quad \text{for the model 1066A}$$

$$0.129 < \alpha < 0.186 \quad \text{for the model PREM} .$$

§ 2. Effect of physical dispersion

Anelasticity induces what is called physical dispersion and we must modify the real part of rigidity by the following formula (ANDERSON & MINSTER, 1979 with correction by SMITH & DAHLEN, 1981).

$$\mu(\sigma)/\mu(\sigma_0) = 1 - \cot(\alpha\pi/2)[(\sigma_0/\sigma)^{\alpha} - 1]/Q_m(\sigma_0) .$$

Thus the real part of Love number k is slightly modified and the Chandler period is lengthend by about 7~11 days (Table 3). Adding 29.8 days of ocean effect to this period explains the observed Chandler period of about 435 sidereal days very well (Table 3).

§ 3. Relation between Q_w and the lower mantle Q_m - energy budget argument

Not a few investigators so far have deduced the relation between Q_w and Q_m from the arguments of energy budgetsa (STACEY, 1977 ; MERRIAM & LAMBECK, 1978). Q_w and Q_m are defined as

$$\begin{aligned} Q_w &= 2E_w/\Delta E \\ Q_m &= 2E_s/\Delta E \end{aligned} \tag{6-11}$$

where E_w is the wobble energy which includes the kinetic, the strain and the gravitational energies. E_s is the strain energy. ΔE is the amount of energy dissipated in one cycle. We should define the kinetic wobble energy E_k as the difference between the kinetic energy in the wobble state and that in the uniform rotation state when the wobble is completely damped.

$$\begin{aligned} E_k &= E_k^w - E_k^u \\ &= (1/2) \sum I_{ij}{}^w \omega_i{}^w \omega_j{}^w - (1/2) \sum I_{ij}{}^u \omega_i{}^u \omega_j{}^u \end{aligned} \tag{6-12}$$

where superscript w and u designate the wobble state and the uniform rotation state, respectively. I_{ij} is the moment of inertia tensor.

Angular velocity vector $\vec{\omega}$ in each state is given by

$$\begin{aligned}\vec{\omega}^{\mathrm{w}}&=\Omega(m_1, m_2, 1+m_3)\\ \vec{\omega}^{\mathrm{u}}&=\Omega(0, 0, 1)\,.\end{aligned} \tag{6-13}$$

Note the difference of reference frames in the two states. MacCullargh's formula gives I_{ij} as

$$I_{ij}{}^{\mathrm{w}}=I\delta_{ij}+(ka^5/3G)(\omega_i{}^{\mathrm{w}}\omega_j{}^{\mathrm{w}}-|\vec{\omega}^{\mathrm{w}}|^2\delta_{ij}) \tag{6-14}$$

$$I_{ij}{}^{\mathrm{u}}=I_{ij}{}^{\mathrm{w}}(m_1=m_2=m_3=0)$$

where $I=(I_{11}+I_{22}+I_{33})/3$ is the inertia of the sphere in the absence of rotational deformation. G and a are the gravitational constant and the Earth's radius, respectively.

Conservation of angular momentum relates m_3 to m_1 and m_2 through

$$(I_{33}{}^{\mathrm{u}}\Omega)^2=\Sigma(\Sigma I_{ij}{}^{\mathrm{w}}\cdot\omega_j{}^{\mathrm{w}})^2\,. \tag{6-15}$$

Observed m_1 and m_2 are of order $0''.2\sim10^{-6}$ and we assume $m_3\sim(m_1{}^2+m_2{}^2)\sim10^{-12}$, which is to be confirmed a posteriori. If we neglect terms much less than 10^{-12}, substituting (6-13) and (6-14) into (6-15) yields

$$m_3=-(m_1{}^2+m_2{}^2)/2\,. \tag{6-16}$$

We can now calculate E_k by combining (6-12) through (6-16) and the result is

$$E_k=0$$

which means $E_k/(I\Omega^2)$ is much less than 10^{-12}.

$$E_k\sim(I\Omega^2/2)\varepsilon\sim10^{18}\,\mathrm{erg} \tag{6-17}$$

with ε of order 10^{-18} or less.

The above expression is at least 10^{-3} times smaller than that given by MERRIAM & LAMBECK (1979). This is because they failed to appreciate the significant difference between $I_{ij}{}^{\mathrm{w}}$ and $I_{ij}{}^{\mathrm{u}}$.

The strain and the gravitational energies due to the deformation of the mantle by the solid pole tide are calculated by the following formula (KOVACH & ANDERSON, 1967 ; TAKEUCHI & SAITO, 1972).

$$E_{\mathrm{s}}=B\int[(ry_2)^2/(\lambda+2\mu)+6(ry_4)^2/\mu+(3\lambda+2\mu)Y^2+24\mu y_3{}^2]dr$$

$$E_{\mathrm{g}}=B\int[-2\rho gry_1Y+3\rho ry_5(y_1-2y_3)-\rho r^2y_1y_6]dr$$

where

$$B=(3/5)(\Omega^2/3)^2\cdot(m_1^2+m_2^2)$$

$$Y=2y_1-6y_3$$

y_j are normalized functions to the unit tidal potential. Performing the integrals for the models 1066A and PREM, we get

$$\begin{aligned} E_s&=7.0\times10^{32}(m_1^2+m_2^2)\ \text{erg}\sim10^{21}\ \text{erg}\\ E_g&=7.7\times10^{32}(m_1^2+m_2^2)\ \text{erg}\sim10^{21}\ \text{erg}\,. \end{aligned} \tag{6-18}$$

Substituting (6-17) and (6-18) into (6-11), we obtain

$$\begin{aligned} Q_w&=(E_w/E_s)Q_m\\ &=2.1\ Q_m \end{aligned}$$

Q_w/Q_m is nearly equal to the value of 1.5 derived in § 1 from the more rigorous argument and the result is satisfying since we have ignored the minor effect of the core in the above discussion. An earlier estimate of $Q_w/Q_m\sim10$ is most likely to be due to the overestimate of E_k by 10^3.

7. Discussion and conclusions

We have resolved three principal problems about the Chandler wobble. The first is the time-variability of the Chandler period. We have tested most of the observational grounds of the variable period hypothesis and found none of them to be definitive. We have shown that "evidence" for the variable period hypothesis is also explained by the model of a invariant Chandler period with a low Q_w. Hence, there is no positive evidence for the variable period model. Although it is impossible to reject the hypothesis in this way, principle of parsimony tells us that the time-invariant Chandler period model is superior to the variable one. The matter becomes obvious if one counts the number of parameters needed to specify each model. The invariant period model requires two parameters (period and Q_w) while the variable period model needs at least another two. They are the modulation magnitude and the modulation period if the Chandler motion is sinusoidally frequency-modulated. More general variable period models require more than four parameters. Since we see no advantage in the variable period model, the model with less parameters is preferred. We believe that the apparent variability of the Chandler period originates in ignorance of stationarity of a time series. As was discussed in § 2 of Chapter 2, we must have records longer than about 50 years in order to secure the stationarity of the time series. However, most of the advocates of the variable period hypothesis drew conclusions

from observations of less than 10 years.

In order to test the hypothesis more directly, we traced the temporal variation of the instantaneous power spectrum of the Chandler wobble. We extended the instantaneous frequency analysis to be applicable to a complex-valued time series for this purpose. We showed that the method has a high resolution and fidelity to trace the evolution of the spectral structure of the polar motion. When applied to IPMS and BIH data for 18 years observation, we did not find any significant fluctuation of the Chandler period. Thus we still support the time-invariant Chandler period model.

The second problem on the Chandler wobble is the wide discrepancy between the earlier estimates of Q_w (Table 2). Now that we saw no observational difficulty in the time-invariant Chandler period model, we may safely estimate Q_w from the Maximum Entropy Spectral Analysis (MESA). We treated the spectrum obtained by MESA from quite a different point of view. We positively exploited the apparent defect of MESA of dependence of the estimated Q_{app} on the prediction error filter length L. First, we observed the behavior of $Q_{app}(L)$ for synthetic polar motion with various Q_w's. Next we compared the result with that obtained from the actual polar motion data. The procedure may appear too simplistic but it yielded the most reliable estimate of Q_w by MESA. A natural Q_w of $50\sim100$ was found to explain the observed behavior of $Q_{app}(L)$ both for ILS and IPMS data. In the estimation process, we found the result by GRABER (1976) of $Q_w=600$ is a product of erroneous choice of L. Our conclusion of $50<Q_w<100$ supported the results of JEFFREYS (1968), WILSON & HAUBRICH (1976a) and OOE (1978).

What is interesting to us is that $50\lesssim Q_w\lesssim 100$ also explains the apparent variable Chandler period very well. The multiple Chandler period detected by GAPOSCHKIN (1972) is explained by the model of $50\lesssim Q_w\lesssim 100$ (Fig. 6). Fluctuation of the Chandler frequency reported by SEKIGUCHI (1972, 1976) is also well explained by the model of $Q_w=100$ (Figs. 8, 9). Variation of the Chandler period presented by GRABER (1976) is explained by $Q_w=50$ (Fig. 11). Thus Q_w of $50\sim100$ explains almost all the "evidence" for the variable Chandler period excellently.

The third problem is the relation between the mantle Q_m and the wobble Q_w. We succeeded in deriving the theoretical Q_w for the realistic Q_w structure by slightly modifying the theory of SASAO, OKUBO & SAITO (1980). In practice, we compute the complex Chandler frequency from the complex Love number arising from the anelasticity of the mantle. We used Rayleigh's principle in order to calculate the small variation of k due to the small imaginary part of elastic moduli. Theoretical Q_w for the frequency-independent Q_m model was found to be about 1.5 times larger than the lower mantle Q_m. The result disagreed with the earlier estimate

of $Q_w/Q_m \sim 10$ derived from the energetic arguments (STACEY, 1969, 1977; MERRIAM & LAMBECK, 1979). We showed that previous authors overestimated the kinetic wobble energy by a factor more than 10^3. We arrived at the conclusion that Q_w/Q_m is at most 2 from the careful argument of the energy budget.

If the wobble energy is totally dissipated in the mantle, we must assume the frequency dependence of Q_m in order to explain the observed Q_w of 50~100. If we assume the power law as the frequency dependence, the power exponent α is found to be in the range of

$$0.143 < \alpha < 0.201 \quad \text{for the model 1066A}$$

$$0.129 < \alpha < 0.186 \quad \text{for the model isotropic PREM.}$$

Physical dispersion due to the anelasticity of the mantle lengthens the theoretical Chandler period of about 402 days (oceanless, perfectly elastic Earth) by 7~11 days. Adding 29.8 days of the ocean effect to this period, we obtain the theoretical Chandler period of 438~443 sidereal days, which agrees with the observed one.

We have neglected the effect of the ocean pole tide on the Chandler wobble in most of the above discussions. However, the ocean effect is clearly important as kinematically suggested by DICKMAN (1979). We should focus our attention on the pole tide in the open sea in the near future.

Acknowledgments

The author wishes to express his sincere thanks to Prof. M. Saito for his encouragement and advice during the course of this study. He also expresses his coordial thanks to Prof. N. Sekiguchi for critically reading the manuscript and making a lot of invaluable comments. The author is indebted to Mr. K. Kurita for his valuable comments in the early stage of this work.

References

AKAIKE, H., 1969, Fitting autoregressive models for prediction, *Ann. Inst. Statist. Math.*, 21, 243-247.

AKAIKE, H., 1969, Power spectrum estimation through autoregressive model fitting, *Ann. Inst. Statist. Math.*, 21, 407-419.

AKAIKE, H., 1970, Statistical predictor identification, *Ann. Inst. Statist. Math.*, 22, 203-217.

ANDERSON, D.L. & J.B. MINSTER, 1979, The frequency dependence of Q in the Earth and implications for mantle rheology and Chandler wobble, *Geophys. J. Roy. astr. Soc.*, 58, 431-440.

BLACKMAN, R.B. & J.W. TUKEY, 1958, *The Measurement of Power Spectra*, Dover, New York.

BUREAU INTERNATIONAL de l'HEURE, 1979, *Annual Report for 1978*, Paris.
BUREAU INTERNATIONAL de l'HEURE, 1980, *Annual Report for 1979*, Paris.
BURG, J.P., 1967, Maximum entropy spectral analysis, *paper presented at the 37-th Meeting, Society of Exploration Geophysicists, Oklahoma City, October 1967.*
BURG, J.P., 1968, A new analysis technique for time series data, *paper presnted at NATO Advanced Study Institute of Signal Processing with Emphasis on Underwater Acoustics, Enshede, Netherlands, August 1968.*
CARTER, W.E., 1981, Frequency modulation of the Chandlerian component of polar motion, *J. Geophys. Res.*, **86**, 1653-1658.
CHANDLER, S.C., 1892, On the variation of latitude, *Astron. J.*, **267**, 17-22.
CLAERBOUT, J.F., 1969, Frequency mixing in Chandler wobble data, *Trans. Am. Geophys. Un.*, **50**, 119.
COLOMBO, G. & I.I. SHAPIRO, 1968, Theoretical model for the Chandler wobble, *Nature*, **217**, 156-157.
CURRIE, R.G., 1974, Period and Q_w of the Chandler wobble, *Geophys. J. Roy. astr. Soc.*, **38**, 179-185.
CURRIE, R.G., 1975, Period, Q_p and amplitude of the pole tide, *Geophys. J. Roy. astr. Soc.*, **43**, 73-86.
DAHLEN, F.A., 1976, The passive influence of the ocean upon the rotation of the Earth, *Geophys. J. Roy. astr. Soc.*, **46**, 363-406.
DICKMAM, S.R., 1979, Consequences of an enhanced pole tide, *J. Geophys. Res.*, **84**, 5447-5456.
DZIEWONSKI, A.M. & D.L. ANDERSON, 1981, Preliminary reference Earth model, *Phys. Earth. Planet. Inter.*, **25**, 297-356.
GAPOSCHKIN, E.M., 1972, Analysis of pole position from 1846 to 1970, in *Rotation of the Earth*, pp. 19-32. D. Reidel Publ. Comp., Dordrecht
GILBERT, F. & A.M. DZIEWONSKI, 1975, An application of normal mode theoty to the retrieval of structural parameters and source mechanisms from seismic spectra, *Phil. Trans. Roy. Soc. London A*, **278**, 197-269.
GRABER, M.A., 1976, Polar motion spectra based upon Doppler, IPMS and BIH data, *Geophys. J. Roy. astr. Soc.*, **46**, 75-85.
GRIFFITHS, L.J., 1975, Rapid measurement of digital instantaneous frequency, *IEEE Trans. Acoust., Speech and Signal Processing*, **ASSP-23**, 207-222.
JEFFEREYS, H., 1968, The variation of latitude, *Mon. Not. Roy. astr. Soc.*, **141**, 255-268.
KIMURA, H., 1918, Variations in the fourteen month's component of the polar motion, *Mon. Not. Roy. astr. Soc.*, **78**, 163-167.
KOVACH, R.L. & D.L. ANDERSON, 1967, Study of the energy of the free oscillations of the Earth, *J. Geophys. Res.*, **72**, 2155-2168.
LACOSS, R.T., 1971, Data adaptive spectral analysis methods, *Geophys.*, **36**, 661-675.
LAMBECK, K., 1980, *The Earth's Variable Rotation*, §5, Cambridge Univ. Press, London.
MELCHIOR, P.J., 1954, Contribution à l'étude des mouvements de l'axe instané de rotation par rapport au Globe terrestre, *Observatoire Royal de Belgique, Monographie* No. 3.
MELCHIOR, P.J., 1957, Latitude variation, in *Physics and Chemistry of the Earth*, **2**, pp. 212-243, Pergamon, New York.
MERRIAM, J.B. & K. LAMBECK, 1979, Comments on the Chandler wobble *Q*, *Geophys. J. Roy. astr. Soc.*, **59**, 281-286.
MUNK, W.H. & G.J.F. MACDONALD, 1960, *The Rotation of the Earth*, §§ 1-10, Cambridge Univ. Press, London.
NEWCOMB, S., 1892, Remarks on Mr. Chandler's law of variations of terrestrial lati-

tudes, *Astron. J.*, 271, 49-50.

O'CONNELL, R. J. & A. M. DZIEWONSKI, 1976, Excitation of the Chandler wobble by large earthquakes, *Nature*, 262, 259-262.

OKUBO, S. & S. TSUBOI, 1982, A new technique for the group velocity analysis of dispersive seismic waves, in preparation.

OOE, M., 1978, An optimal complex AR. MA model of the Chandler wobble, *Geophys. J. Roy. astr. Soc.* 53, 445-457.

PEDERSEN, G. P. H. & M. G. ROCHESTER, 1972, Spectral analyses of the Chandler wobble, in *Rotation of the Earth*, pp. 33-38, D. Reidel Publ. Comp., Dordrecht

POLLACK, L. W. & A. HANEL, 1935, Bericht über die numerische Methode von J. Fuhrich zur Ermittlung von Periodizitäten, *Meteorologische Zeitschrift*, 52, 330-333.

ROCHESTER, M. G., 1973, The Earth's rotation, *Trans. Am. Geophys. Un.*, 54, 769-781.

RUDNICK, P., 1956, The spectrum of the variation in latitude, *Trans. Am. Geophys. Un.*, 37, 137-142.

SASAO, T., S. OKUBO & M. SAITO, 1980, A simple theory on the dynamical effects of a stratified fluid core upon nutational motion of the Earth, in *Nutation and the Earth's Rotation*, pp. 165-183, D. Reidel publ. Comp., Dordrecht.

SAITO, M., 1978, An automatic design algorithm for band selective recursive recursive digital filters, *Butsuritanko (Geophysical Exploration)*, 31, 112-135.

SEKIGUCHI, N., 1961, On the strong coupling between the mantle and the core of the Earth, *Publ. Astron. Soc. Japan*, 13, 23-50.

SEKIGUCHI, N., 1966, On the damping coefficient of the polar motion, *Publ. Astron. Soc. Japan*, 18, 116-126.

SEKIGUCHI, N., 1972, On some properties of the excitation and damping of the polar motion, *Publ. Astron. Soc. Japan*, 24, 99-108.

SEKIGUCHI, N., 1976, An interpretation of the multiple-peak spectra of the polar wobble of the Earth, *Publ. Astron. Soc. Japan*, 28, 277-291.

SMITH, M. L., 1974, The scalar equations of infinitesimal elastic-gravitational motion for a rotating, slightly elliptical Earth, *Geophys. J. Roy. astr. Soc.*, 37, 491-526.

SMITH, M. L., 1977, Wobble and nutation of the Earth, *Geophys. J. Roy. astr. Soc.*, 50, 103-140.

SMITH, M. L. & F. A. DAHLEN, 1981, The period and Q of the Chandler wobble, *Geophys. J. Roy. astr. Soc.*, 64, 223-281.

SMYLIE, D. E., G. K. C. CLARKE & T. J. ULRYCH, 1973, Analysis of irregularities in the Earth's rotation, in *Methods in Computational Physics*, 13, pp. 391-430, Academic Press, New York.

STACEY, F. D., 1969, *Physics of the Earth*, 1-st Edn., §§ 2, 7, John Wiley & Sons, New York.

STACEY, F. D., 1977, *Physics of the Earth*, 2-nd Edn., §§ 3, 10, Jonn Wiley & Sons, New York.

TAKEUCHI, H. & M. SAITO, 1972, Seismic surface waves, in *Methods in Computational Physics*, 11, pp. 217-295, Academic Press, New York.

ULRYCH, T. J., 1972, Maximum entropy power spectrum of truncated sinusoids, *J. Geophys. Res.*, 77, 1396-1400.

ULRYCH, T. J., D. E. SMYLIE, O. G. JENSEN & G. K. C. CLARKE, 1973, Predictive filtering and smoothing of short records by using maximum entropy, *J. Geophys. Res.*, 78, 4959-4964.

ULRYCH, T. J. & T. N. BISHOP, 1975, Maximum entropy spectral analysis and autoregressive deconvolution, *Rev. Geophys. Space Phys.*, 13, 183-200.

WIDROW B. & M. E. HOFF, 1960, Adaptive switching circuits, in *IRE 1960 Wescon Conv. Rec.*, part 4, 96-104.

WILSON, C.L. & R.A. HAUBRICH, 1976a, Meteorological excitation of the Earth's wobble, *Geophys. J. Roy. astr. Soc.*, **46**, 707-743.

WILSON, C.L. & R.A. HAUBRICH, 1976b, Atmospheric contribution to excitation of the Earth's wobble 1901-1970, *Geophys. J. Roy. astr. Soc.*, **46**, 745-760.

YUMI, S., 1970, Stability of station and the Earth's figure, in *Earthquake Displacement Fields and the Rotation of the Earth*, pp. 63-68, D. Reidel Publ. Comp., Dordrecht.

YUMI, S., 1980, *Annual Report of the International Polar Motion Service for the year 1978*, Mizusawa.

YUMI, S. & K. YOKOYAMA, 1890, *Results of the International Latitude Service in a homogeneous system 1899.0-1979.0*, Mizusawa.

---

1. チャンドラー極運動の周波数変調仮説の検定とそのQに関する研究

東京大学理学部　大久保修平

チャンドラー極運動は地球の elastic-gravitational な自由振動の一つのモードであり，瞬間自転軸が形状軸のまわりを反時計回りに回転する極運動である．その周期は約435日であり，他の地震学的なモードの周期よりも 10^4 倍以上も長いという特徴がある．したがって，その Q 値はマントルの非弾性的性質，とりわけ周波数依存性を議論する上できわめて重要となる．また地球科学の諸分野（地震学，海洋学，気象学，地球電磁気学）とチャンドラー極運動の関りの上でも Q を確定することは大切になってくる．

ところでチャンドラー極運動の Q（以下 Q_w と記す）を議論する前に片付けておかねばならない懸案がある．それはチャンドラー極運動が周波数変調を受けているという仮説の検定である．この仮説は過去90年にわたって論争されてきたが，未だその当否は確定していない．この仮説が正しいとするならば，通常のスペクトル解析等から求めた Q（以下 Q_{app} と記す）とチャンドラー自由振動の減衰を表わす Q_w とは全く対応しなくなる．したがって Q_{app} をもって Q_w の推定値としてきた従来の解析結果の根底が揺るがされる恐れがある．

本研究では，以下の二通りの方法で周波数変調仮説を検定した．

（I）非定常時系列の瞬間パワースペクトルという概念を複素時系列にも適用できるように拡張した．この解析手段を使って最近20年間のチャンドラー周波数の時間変化を追跡した．

（II）周波数変調仮説の根拠とされる解析結果の検討．まず周波数変調を受けていない極運動モデルを仮定し，シミュレーションデータを合成する．この合成記録から，見かけ上は周波数変調を示す結果が得られないかどうか数値実験する．

（I）の解析から，極運動が周波数変調を受けているとしても±1%程度であり，この値は有意とはみなされないことが明らかになった．さらに驚くべきことに（II）から，周波数変調仮説の根拠とされていた従来の解析結果のすべてが，チャンドラー周期一定のモデルでも説明できることがわかった．したがって周波数変調仮説を積極的に支持する根拠はなくなったと言える．

以上のことから Q_w をスペクトル解析から求めても支障がないことが確められた．ところが Q_{app} は研究者によって推定値が異なり，10～600という幅を持っている．本研究の第二の目的は，Q_w の推定値がこのように混乱している原因を明らかにし，正しい Q_w の値を求めることである．解析手段として，スペクトル分解能，安定性の優れた Maximum Entropy Method を採用した．prediction error filter の長さ L に Q_{app} が依存するという MEM の欠点を逆に利用して $Q_{app}(L)$ から Q_w を求めることに成功した．手続きとしては，まずさまざまな Q_w 値を仮定して極運動のシミュレーションデータを合成する．次にそれぞれの合成記録について $Q_{app}(L)$ を求め，それを実際の極運動データから得られた $Q_{app}(L)$ のグラフと比較する．最も良い一致を見せた $Q_{app}(L)$ のグラフから Q_w を推定することができる．その結果，$50 \leqq Q_w \leqq 100$ であることが ILS(70年間) と IPMS (15

年間）のデータから明らかにされた．同じ MEM を用いて得られていた $Q_w=600$ という結果は，不適切な L に対応した Q_{app} をもって Q_w の推定値としたためであることが分った．MEM 以外の方法で解析された $Q_w \leqq 50$ という結果は，方法自体の周波数分解能が低いために導かれた見かけ上の結果であることもわかった．

本研究の第三の目的はマントルの非弾性的性質とチャンドラー極運動の Q および周期との関係を議論することである．まずマントルの Q（以下 Q_m と記す）と Q_w の関係を導くためには，非弾性地球のチャンドラー角周波数 $\tilde{\sigma}_c$（複素数）を理論的に求める必要がある．本研究では，完全弾性地球からの摂動として，非弾性地球モデルをとらえ，弾性定数の摂動（複素数）に対するチャンドラー角周波数 σ_c の変分（複素数）を計算した．実際には σ_c はラブ数 k の関数であるから，k の変分 δk（複素数）を求めればよい．normal mode の解が満たすエネルギー積分の恒等式に Rayleigh's principle を適用することにより δk を求め，$\delta\tilde{\sigma}_c$ を計算することができた．$\delta\sigma_c=\tilde{\sigma}_c-\sigma_c$ の虚数部は極運動の減衰を表わすので Q_w と関係づけることができる．Q_w とチャンドラー周期における Q_m の間に

$$Q_w \sim 1.5\, Q_m(\sigma=\sigma_c)$$

という関係が示された．Q_m の周波数依存性を

$$Q_m(\sigma) \propto \sigma^{\alpha}$$

と仮定すると，$50 \leqq Q_w \leqq 100$ という観測結果を説明するためには，$0.1 \leqq \alpha \leqq 0.2$ でなければならないことが明らかになった．

$\delta\sigma_c$ の実部からは，チャンドラー周期が物理分散によって7～11日のびることがわかった．弾性地球のチャンドラー周期が402日であり，海洋によって周期が30日のびることを考えると，非弾性地球のチャンドラー周期の理論値は438～443日となり観測と良く一致する．